

Response to E. Ray (Referee)

Dear Eric Ray,

Thanks for your constructive and inspiring comments. They helped us a lot to improve the paper. In the following, we address all the points raised by you (denoted by italic letters). Following your (and Gloria Manney's) recommendation, section 5 and related Figures were almost completely revised. To render this response easy to read, you will find your original comments in italic letters, our answers in roman letters and the references to the manuscript (and in the manuscript) are highlighted in red.

This paper describes the NH major sudden warming event of 2009 from a modeling and satellite observation perspective. The CLaMS model provides explicit information about the effects of sub-grid scale mixing and this is used to explain features in the trace gas correlations related to the MW seen in MLS measurements and CLaMS output. The description of the dynamical evolution of the NH stratosphere from the tropics to the pole before and after the MW is interesting and well done. The description of the evolution of the N₂O-O₃ correlations related to this dynamical evolution is important but unfortunately is not described or shown well enough.

I have used tracer correlations extensively and appreciate their value but it took me several readings to understand all of the features described in Section 5. This was due to a combination of not describing all of the features well, not showing the changes in the correlations clearly enough and not giving the reader enough motivation up front to make the effort to follow the description. Tracer correlations are not widely used and understood, even though they are powerful indicators of transport features. Extra help in guiding readers through this section is necessary if you want them to understand what you have done and how useful it is. Consistent translation between physical space and tracer correlation space is required throughout this section.

There are many grammatical errors and I have attempted to list the most obvious ones below. This made the paper difficult to understand in sections. I would suggest the authors perform a detailed grammar review before the paper is resubmitted.

Overall the paper describes interesting work and I suggest it is published after revision of Section 5 and grammatical improvements are made.

We totally agree with the referee that the difficulty in reading section 5 arises from lack of translation between tracer space and physical space and also from the high density of information without proper guidance in the text. To improve this, we revised the paper in the following two ways:

1) One schematic (new Fig. 1) was added to the introduction. This figure and the corresponding description will give the readers the background of tracer- tracer correlations before further in depth analysis.

2) Section 5 has been rewritten, as the main concern of the reviewer. Four subsections are included in section 5: N₂O-O₃ correlations: MLS versus CLaMS; tracer and physical space; isentropic mixing versus cross-isentropic transport; impact of chemistry. Following the recommendation of the reviewer, we combined the original Figure 7 and Figure 9 to a new Figure 9 to get an easier comparison between MLS and CLaMS. To achieve a consistent translation between physical

space and tracer correlation space, the Figure 8 is extended: the physical space interpretations are added to the corresponding tracer correlation. Accordingly, the text of Section 5 is re-organized and revised.

Specific comments

- Pg. 4384, line 8: *using tracer-tracer correlations is not really a “technique”*. I would remove that word and just say *“tracer-tracer correlations and by. . .”*

Changed, see Pg.1 Line 6.

- Pg. 4385, line 26: insert *“the”* before *“Pacific”*

Insert.

- Pg. 4386, line 2: remove *“the”* before *“recent”* and *“10”* after *“recent”*

Changed, see Pg. 2 Line 56.

- Pg. 4386, line 8: change to *“, which describes”* after *“advection”*

Changed, see Pg. 2 Lines 65-66.

- Pg. 4386, line 9: *“along a 3D”*, insert commas after *“trajectory”* and after *“mixing”*. Add *“which parameterizes”*

Changed, see Pg. 2 lines 65-67.

- Pg. 4386, line 10: remove *“the”* before *“air”*

Article is removed.

- Pg. 4386, line 21: remove *“the”* before *“models”*

Article is removed.

- Pg. 4388, line 9: change *“at”* to *“on”*

Changed.

- Pg. 4388, line 14: add *“the”* before *“generation”*

Added.

- Pg. 4388, line 16: add “the” before “disturbance”

Added.

- Pg. 4388, line 22: change “during” to “over”

Changed.

- Pg. 4388, line 25: change “at the end” to “in turn”

Changed, see Pg. 6 line 165.

- Pg. 4391, line 12: change “on” to “in”

Changed.

- Pg. 4393, line 22: change “altitudes” to “altitude”

Changed.

- Pg. 4393, line 23: add “mid-latitude” before “surf zone”

Changed.

- Pg. 4394, line 7: add comma after “easterlies”

Changed.

- Pg. 4394, line 27: Remove “Complementary,” and change “illustrate” to “illustrates”

Changed, see Pg. 10 line 331.

- Pg. 4395, line 1: change “vertex” to “vortex”

Changed.

- Pg. 4395, lines 2 and 3: change “days” to “day”

Changed.

- Pg. 4395, line 24: remove “and” before “after”

Removed.

- Pg. 4396, line 3: add “shown” before “although”

Added.

- Pg. 4396, line 24: add “of” before “picture”, remove “does” and change “respond” to “responds”

Changed, see Pg. 12 lines 380-381.

- Pg. 4396, line 29: change “Another important point is” to “This would help provide”

Changed, see Pg. 12 line 385

- Pg. 4397, line 1: add “of” before “how” and remove “itself”

Changed, see Pg. 12 line 385.

- Pg. 4397, line 5: change “much” to “even” and add “so” after “more”

Changed, see Pg. 12 line 389.

- Pg. 4397, line 9: I’d suggest removing “technique” and just saying “correlations”

Changed, see Pg. 12 lines 392.

- Pg. 4397, line 12: remove “the” after “shows”, change “correlation” to “correlations”, remove “the” before “MLS” and remove “a” before “probability”

Changed, see Pg. 12 lines 396-397.

- Pg. 4397, line 14: change to “data cover the NH eq. latitudes. . .”

Changed.

- Pg. 4397, lines 20-21: change to something like “two stronger branches and one weaker branch of N2O-O3 correlations. . .”

Changed, see Pg. 12 lines 403-404.

- Pg. 4397, lines 22-23: end sentence after “Fig. 7a“. New sentence starts “These branches describe. . .”, change to “. . .within the polar vortex, the surf zone and the tropics. . .”

Changed, see Pg. 12 line 405.

- Pg. 4397, line 25: remove “the” before “tracer-tracer”

Removed.

- Pg. 4398, line 1: remove “the” before “tracer-tracer”

Removed.

- Pg. 4398, line 2: change “Reversely” to “Conversely”

Changed.

- Pg. 4398, line 3: change “at the same time” to “following the MW”

Changed to “in the time period after the MW”.

- Pg. 4398, line 5: change “will be” to “is”

Changed.

- Pg. 4398, line 13: change “Reversely” to “Conversely”

Changed.

- Pg. 4398, lines 20-25: *This paragraph should be rewritten or at least another sentence or two added to make it more clear what you are describing. In line 20 I would change to “. . . range of potential temperatures are considered. . .”*

This paragraph was rewritten.

- Pg. 4399, lines 14 and 15: remove “Similar”, remove “same”, add comma after “before”

This paragraph was rewritten according to the new combined Figure 9.

- Pg. 4399, lines 16-22: *Need to more clearly explain why the tropical latitudes are excluded in the correlation plots. Also, should explain more clearly that the tropical correlation is seen in the non-mixing run because of the tropical air that has physically moved into the mid-latitudes and not been mixed. It helps to relate physical space to tracer correlation space as clearly as possible so readers can translate between the two more easily.*

The new Figure 9 is marked with the latitude range more clearly. And the Subsection 5.3.1 “transport 415 from the tropics” explain this point.

- Pg. 4400, lines 1-2: *This is really for the whole paragraph but you need to more clearly show in Figure 9 how the non-mixing correlations cannot be reconciled with observations. I have more suggestions on how to change the figures below.*

We follows the suggestions to improve the figure.

- Pg. 4400, line 3: change “trajectories” to “trajectories”

Changed.

- Pg. 4400, lines 8-10: *The isentropes move upward in tracer space but not in physical space. This is another place where you should be clear so that it is easier to translate between what is happening in physical vs. tracer correlation space.*

We agree this sentence is not clear. So we add “in tracer space” to address it is not physical vertical moving of isentropes. See Pg. 15 Lines 484-486. And the Figure 1 (b) added in introduction would also prepare the readers about the interpretation of upwelling and downwelling in tracer space.

- Pg. 4400, lines 16-28: *This discussion of Figure 10 and how descent affects the tracer correlations should be moved after the discussion of Figure 9a1-c1 on Pg. 4401. The best flow of the discussion would be to first compare Figure 7 to Figure 9a1-c1 since those correlations should be the most similar. I would also strongly suggest that you combine Figure 7 with Figure 9 so that it is easier to compare the MLS correlations with the CLaMS correlations.*

We totally agree. The Figure 7 and 9 were combined, and Section 5 is re-organized.

- Pg. 4401, line 1: *What does “very similar” refer to here? Similar to what?*

The original statement “very similar” refers to the similarity of MLS tracer- tracer correlation with CLaMS tracer- tracer correlation. Since the Figure 7 and 9 are combined and text is revised, please check the text of Section 5.1.

- Pg. 4401, lines 7-8: *Not sure what is meant by the mid-latitudes “do not undergo further descent”. There is descent in the mid-latitudes all winter is not there?*

The text here brought some misunderstanding. With “do not undergo further descent” we meant: the APs spread from polar region to mid-latitudes still stay inside the considered vertical range even with persistent descent during winter. So we changed the sentence accordingly. See Pg. 15 Line 512.

- Pg. 4401, lines 11-12: *The effects mentioned here are not well discerned in Fig. 9. The changes in the correlations are subtle on plots of this size so lines need to be added to better compare between them. You could add the three main branches in Fig. 9a1-c1 onto 9a2-c2. You could add the main branches in MLS onto Fig. 9a1-c1. Something like this needs to be done to make the subtle shifts in the correlations more obvious.*

For better comparison between CLaMS run with and without mixing and to emphasize the effect of mixing, the dashed black curves were added to Fig. 9 (a2-c2) which show the estimated N₂O-O₃ correlation line from the case without mixing (i.e. from a3-c3). Reversely,

dashed lines in Fig. (a3-c3) are schematically transferred correlation branches from CLaMS with mixing (i.e. from a2-c2).

- Pg. 4401, line 14: change “(by far more)” to “mostly”, “mid-latitude” is misspelled, add “some” before “tropical”

Changed. See [Pg.16, L.519-520](#).

- Pg. 4401, lines 19-21: Again, this slight shift is too hard to see in the figure. Need to add some lines to help guide the reader.

The corresponding correlation lines are added in Figure 9. The dashed black curves in (a2-c2) show the estimated N2O-O3 correlation line from the case without mixing (i.e. from a3-c3). Reversely, dashed lines in (a3-c3) are schematically transferred correlation branches from CLaMS with mixing (i.e. from a2-c2).

- Pg. 4402, lines 2-5: This sentence is too long, needs to be broken up. Also, what are the “highest values” that are referred to here?

The long sentence has been re-organized. See [Pg. 16 Lines 530-533](#). The “highest values” are referred to **high (increased) values of NOx chemistry**.

- Pg. 4402, line 6: change to “warm winter in 2008/09, few PSCs. . .”, remove “subsequent,”

Changed.

- Pg. 4402, line 21: change “the” to “a”, change “latitude” to “location”

Changed. See [Pg. 16 L.546](#).

- Pg. 4402, line 25: change to “detail similar to Crutzen. . .”

Changed to “ as defined by Crutzen...”.

- Pg. 4403, line 1: remove “other”

Removed.

- Pg. 4403, line 3: change “Contrary” to “In contrast”

Changed. See [Pg. 17 L.556](#).

- Pg. 4403, line 4: change to “a most probable location of”

Changed. See [Pg. 17 L.557](#).

- Pg. 4403, line 8: change “here” to “in this part of the tropics”

Changed. See L. 560.

- Pg. 4403, line 9: change to “investigated whether the”, change “has” to “had”

Changed. See L. 561.

- Pg. 4403, line 23-24: change to “which resulted”, “upwelling through late March”

Changed. See L. 574.

- Pg. 4404, lines 8-9: change to “MW, triggered by”

Changed. See L. 585.

- Pg. 4404, line 10: add “been” after “have”

Changed. See L. 587.

- Pg. 4404, line 20: change “the order of” to “a”

Changed.

- Pg. 4404, line 24: add “us” after “allow”

Added.

- Pg. 4404, lines 26-27: remove “a” before “significant”, add comma after “loss”

Changed. See Pg. 18 Lines 602-603.

- Pg. 4405, line 12: remove “exemplary”

Removed.

- Pg. 4405, line 15: change to “correlation, which disappears. . .”

Changed. See Pg. 18 L. 618.

- Pg. 4405, lines 21-22: change to “is it the N₂O or the. . .”, “an impression of how. . .”

Changed. See Pg. 18 Line 623.

- *Pg. 4406, lines 1-4: remove “Complementary,” end first sentence with “are also used.” Then start with “An ACE profile crossed the potential temperature surfaces. . .on this day (red circles are the profile. . .”. Remove “as well as the corresponding CLaMS profiles before and after applying the averaging kernel”*

Changed. See [Pg. 19 Lines 630-632](#).

- *Figures 7 and 9 should be combined so that the MLS correlations are on the top row and it is easy to compare among all the correlation plots. Clearly label on the left side of each row that it is MLS, CLaMS with mixing and CLaMS without mixing. Add correlation lines from similar plots such as was done in Fig. 11 for easier comparison.*

Figures 7 and 9 have been combined to a new Figure 9 with side-labels. The correlation lines are added to middle and bottom panels derived from each other. Please see [Figure 9](#) and the corresponding text in [Section 5.1](#).

- *Figure 12: Why is the bottom right plot so different from Fig. 9c1 or 9b1? Those plots are all from a similar time period and the plots in Fig. 9 do have a polar correlation.*

It is because the Fig. 9 (last version) used all the APs of CLaMS in a certain window while Figure 12 (last version) used the CLaMS APs interpolated to the corresponding MLS observations. The interpolation is done by collecting nearest neighbor APs to the corresponding observation. Thus, the number of the CLaMS APs in Figure 12 is much less than Figure 9. The detail of the interpolation is written in [Section 3.2](#).

Response to Anonymous Referee

Can the authors give an estimation about the influence of the type of this specific 2009 MW (vortex split) on the results? Is it possible to generalise the results, i.e. is the analysing method (tracer-tracer correlations) sensitive enough to be applicable also to MWs which are less intense than the exceptionally strong 2009 MW?

It is possible and even easier to apply tracer-tracer correlations on a less intensive MW. Because the main difficulty of analyzing tracer-tracer correlations is distinguishing the dynamical effect (advection and mixing) from chemistry (e.g. chlorine-induced ozone loss, NO_x chemistry). A winter with stable and cold polar vortex (or with a less intense warming) indicates less transport or mixing across the transport barriers, which is favorable for the compact tracer-tracer correlations and thus the chemistry effect is possibly dominant. In fact, ozone-tracer relations have been used extensively to estimate ozone loss (e.g., Proffitt *et al.*, 1990; Müller *et al.*, 1996, 2001; Tilmes *et al.*, 2006). However, the intensive 08/09 MW case is an example that dynamics and chemistry is mixed up in tracer space. Therefore, special attention should be paid on applying tracer-tracer correlations. In this sense, a chemical transport model with explicit mixing process will help us to understand the details of the tracer-tracer correlations.

In order to explain this point better and also following the other referees' recommendations, we revised considerably the introduction and Section 5. One schematic (new Fig. 1) was added to the introduction. This figure and its corresponding text give the background of tracer-tracer correlation before further discussion. Then section 5 was re-organized into four subsections: N₂O-O₃ correlations: MLS versus CLaMS; tracer and physical space; isentropic mixing versus cross-isentropic transport; impact of chemistry. To achieve a consistent translation between physical space and tracer correlation space, the Figure 8 is extended: the physical space interpretations are added to the corresponding tracer correlation.

Specific comments

- *Page 4386, line 8:*
Your description of atmospheric transport refers to the modelling perspective of this process. This should be emphasised in this context.
We modified the paragraph.
See [L.65-68 on Page 3](#).
- *Page 4386, line 6:*
Are the result of Sofieva et al. (2012) related only to a specific MW (if yes, which one?), or are these results obtained by analysing several MWs?
Sofieva *et al.* (2012) studied four SSWs (2002- 2003, 2003- 2004, 2005- 2006 and 2007-2008) and three SSWs (2003 Jan, 2004 Jan and 2006 Jan) met the criteria of MWs.
- *Page 4388, lines 4-6:*
Unlike you have stated, a negative temperature gradient between the North Pole and 60° Nat 10 hPa is characteristic for an undisturbed polar vortex. This situation is present during the second half of December 2008 and the first half of January 2009.
You should start with a more general statement about the stratospheric winter 2008/09, instead of starting with a sentence about the Minor warming, which is present during the

first week of December 2008, indicated by a slightly positive temperature difference between the North Pole and 60°N at 10 hPa and a deceleration of the stratospheric jet.

We agree. The description of minor warming is “second order” information and somehow miss-leading. And another reviewer also pointed this out and suggested us to clarify the definition of major SSW here. Therefore, we rewrote the paragraph with a general statement: major SSW criteria we used and the central date identification.

- *Page 4391, lines 19-23:*

description of model runs; You should try to reformulate this section, to clarify your experimental setup. As far as I understood this paragraph, you performed two simulations with CLaMS, one with mixing and one without mixing. Both simulations are performed with full chemistry, and in both simulations, besides the ozone calculated with full chemistry, also a passive ozone tracer is present.

Or have there been four different CLaMS simulations: two sets of simulations, first set (full chemistry) with mixing and without mixing, second set (passive ozone tracer) with mixing and without mixing.

A table, summarizing the experimental setup with unique labels for each simulation would be helpful. Using these labels consequently in section 5 could help the reader to better follow your argumentation.

The two simulations both with O₃ as passive tracers are performed in our studies. The difference of these two runs is including mixing or not. To say it more clearly, we revised **the last paragraph in Section 3.1**.

- *Page 4395, line 6:*

Please give a short description of the Nash criterion here.

The description of the Nash criterion is added here and also in Figure 4 caption.

See **L.300-303 on Page 9 and caption of Fig. 4 (original Fig. 3)**.

- *Page 4402, lines 8-11:*

chlorine induced ozone loss; More explanation is needed here to follow your argumentation. Figure 7a (situation from December 18-28) and 7b (situation from January 18-28) both display situations during mid-winter. How can these figures be used to analyze the chlorine induced ozone loss, mainly occurring in late winter and spring?

Firstly, the new Fig. 1 (c) might be helpful to illustrate how to use ozone-tracer correlations to examine polar ozone loss. Secondly, the chlorine driven polar ozone loss usually happens in the late winter and early spring within a sufficiently cold polar vortex. However, a new study by *Manney et al.* (2015) has confirmed that the ozone loss was significant due to the unusual low temperature in the lower stratospheric polar vortex before the MW (mainly in December and January) in a very similar strong MW winter (2012/13). Some changes has been included in the Section 5.4 about this point.

Technical corrections

- *Page 4385, line 26: insert article; ... over the Pacific.*
Article is inserted.
- *Page 4385, line 26: delete article ; ... before the MW and strongest after ...*
Article is deleted.
- *Page 4386, line 1: delete article ; ... trend of occurrence of NH MWs ...*
Article is deleted.
- *Page 4388, line 11: insert article; ... the sudden rise of the polar cap temperature ...*
Article is inserted.
- *Page 4388, line 16: insert article; ... while the disturbance of wind and temperature ...*
Article is inserted.
- *Page 4389, line 12: Correct the unit for the eddy heat flux to $K m s^{-1}$*
Corrected.
- *Page 4389, line 13: date format changes; Change 6 January to January 6. Also change the date format in line 13 and 14 on the same page and at subsequent pages, to be consistent.*
Changed.
- *Page 4395, line 1: correct; ... stable vortex ...*
Changed.
- *Page 4417, text displayed within figure 5: To make the information more readable please plot the text within figure 5 in white*
Changed.

References

- Manney, G. L., Z. Lawrence, M. Santee, N. Livesey, A. Lambert, and M. Pitts (2015), Polar processing in a split vortex: Arctic ozone loss in early winter 2012/2013, *Atmospheric Chemistry and Physics*, 15(10), 5381–5403.
- Müller, R., P. J. Crutzen, J.-U. Grooß, C. Brühl, J. M. Russell III, and A. F. Tuck (1996), Chlorine activation and ozone depletion in the Arctic vortex: Observations by the Halogen Occultation Experiment on the Upper Atmosphere Research Satellite, *J. Geophys. Res.*, 101, 12,531–12,554.
- Müller, R., U. Schmidt, A. Engel, D. S. McKenna, and M. H. Proffitt (2001), The O₃–N₂O relationship from balloon-borne observations as a measure of Arctic ozone loss in 1991/92, *Q. J. R. Meteorol. Soc.*, 127, 1389–1412.
- Proffitt, M. H., J. J. Margitan, K. K. Kelly, M. Loewenstein, J. R. Podolske, and K. R. Chan (1990), Ozone loss in the Arctic polar vortex inferred from high altitude aircraft measurements, *Nature*, 347, 31–36.

Sofieva, V., N. Kalakoski, P. Verronen, S.-M. Päivärinta, E. Kyrölä, L. Backman, and J. Tamminen (2012), Polar-night O₃, NO₂ and NO₃ distributions during sudden stratospheric warmings in 2003–2008 as seen by gomos/envisat, *Atmospheric Chemistry and Physics*, 12(2), 1051–1066.

Tilmes, S., R. Müller, A. Engel, M. Rex, and J. Russell III (2006), Chemical ozone loss in the Arctic and Antarctic stratosphere between 1992 and 2005, *Geophys. Res. Lett.*, 33, L20812, doi:10.1029/2006GL026925.

Response to G. Manney (Referee)

Dear Gloria Manney,

Thanks a lot for this extremely thoughtful review that was made in a very constructive spirit; it has encouraged us “to do things better”. In the following, we address all the points raised by you (denoted by italic letters). The second reviewer, Eric Ray, also gave us many very constructive hints which, to some extent, slightly overlap with your comments. Following your (and Eric Ray’s) recommendation, section 5 and related Figures were almost completely revised. To render this response easy to read, you will find your original comments in italic letters, our answers in roman letters and the references to the manuscript (and in the manuscript) are highlighted in red.

General Comments

This paper presents a detailed analysis of transport during the 2009 major sudden stratospheric warming (SSW) using the CLaMS Lagrangian transport model and MLS trace gas data. The detailed analysis of transport is presented primarily by discussing correlations between O₃ and N₂O. This work, and the conclusions drawn from it, is very interesting, presenting a new view of transport during an SSW; the work it describes is appropriate for and should be of substantial interest to the readership of ACP. However, substantial revisions are needed before it is suitable for final publication.

- *The most serious issue is the discussion of tracer correlations in Section 5, which I found it extremely difficult to follow though I have significant experience with the use of tracer correlations. Correlations of ozone and a long-lived tracer such as N₂O have been used in numerous studies, and can be an interesting and informative way to view trace gas data, especially in cases where those data do not offer hemispheric daily coverage and thus transport and chemical processes cannot be diagnosed by examining the day-to-day evolution in physical space. However, interpretation of such tracer correlations is complex, and chemical and transport processes can, in some situations, produce similar changes. In addition, not all of your readers will be familiar with the use and interpretation of tracer correlations. Therefore, a much more complete and systematic description of how various processes affect the tracer correlations, and what that implies for the particular cases shown here, is needed. In fact, I believe the authors are missing an important opportunity here: Because they are using MLS data and a model that both offer full daily hemispheric fields, it is possible to relate the changes in tracer correlations to specific changes in physical space and in time - if done systematically, this would be extremely valuable and would not only clarify the interpretation that is currently given of the tracer correlations, but would serve as a valuable guide to the interpretation of trace correlations in general. I strongly encourage the authors to include such an analysis.*

Yes, we completely agree. In the response to this criticism, section 5 was almost completely rewritten. This section was also subdivided in several sub-section in order to achieve a clearer structure for our arguments. The new Fig. 8 should make it easier to switch between

the physical- and tracer-space. Furthermore, we combined original Fig. 7 and 9 as the new Fig. 9 and included some reference correlation in order to see better the changes in the correlations during the winter.

- *In addition to the very helpful Plumb et al review paper already cited here, several papers that I have found useful for their clear descriptions of the complexities of interpreting tracer correlations are:*

Waugh et al., 1997: Mixing of polar vortex air into middle latitudes as revealed by tracer-tracer scatterplots, JGR.

Michelsen et al., 1998, Correlations of stratospheric abundances of CH₄ and N₂O derived from ATMOS measurements, GRL.

Michelsen, et al., 1998, Correlations of stratospheric abundances of NO_y, O₃, N₂O, and CH₄ derived from ATMOS measurements, JGR.

Plumb, et al., 2000, The effects of mixing on tracer relationships in the polar vortices, JGR.

Esler and Waugh, 2002, A method for estimating the extent of denitrification of Arctic polar vortex air from tracer-tracer scatterplots, JGR.

Ray, et al., 2002, Descent and mixing in the 1999-2000 northern polar vortex inferred from in situ tracer measurements, JGR.

Sankey and Shepherd, 2003, Correlations of long-lived chemical species in a middle atmosphere general circulation model, JGR.

Hegglin and Shepherd, 2007, O₃-N₂O correlations from the Atmospheric Chemistry Experiment: Revisiting a diagnostic of transport and chemistry in the stratosphere, JGR.

In addition to the Plumb (2007) review paper, the last of this list is already cited in the current manuscript. However, the tracer correlation method is sufficiently intricate and dependent on particular circumstances (e.g., patterns of mixing, types and rapidity of chemical processes, spatial/temporal variations in chemical lifetimes and in transport barriers) that a fuller description of the relationships to spatial variations is needed to guide the reader through the interpretation of the correlation plots. Some of these papers may be helpful in accomplishing that.

This review comment again criticizes the discussion of tracer correlations and suggests a more extensive discussion of the literature – in response to this criticism we have considerably expanded the discussion of this point, in particular with a focus on the relation between physical space and tracer space as suggested (see also response above). A new Figure has been added (Fig. 8 in the revised version) and section 5 was rewritten accordingly.

Further, we have added some background material on the impact of different processes on tracer relations in the introduction and added a schematic (new Fig. 1). This serves to give the background to the further discussion later in the paper and will make this material easier to follow. In these discussions, we also refer now to many of the papers suggested (e.g. *Michelsen et al., 1998; Ray et al., 2002; Sankey and Shepherd, 2003; Hegglin and Shepherd, 2007; Plumb, 2007*).

- *The other significant issue I have is that there are several papers that examine three dimensional transport during the 2009 SSW that should be cited and discussed in relationship to*

the results presented here. There are also some papers discussing the meteorology of that winter that are either not cited or for which the current results are not placed in the context of this previous work. One of these papers, Manney et al, 2009, GRL, is cited, but only in the introduction in a general sense - their results discussing the time evolution of MLS trace gas data (including N₂O and the implications of that evolution for mixing) should be related to the results shown here. They also discuss the meteorology during this event, and this should be related to the meteorological discussion in this manuscript. Two other papers with results that should be discussed in the context of the work on transport presented here are:

Orsolini, et al, 2010, Descent from the polar mesosphere and anomalously high stratopause observed in 8 years of water vapor and temperature satellite observations by the Odin sub-millimeter radiometer, JGR.

Lahoz, et al, 2011, The 2009 stratospheric major warming described from synergistic use of BASCOE water vapour analyses and MLS observations, ACP.

The third paragraph of introduction, where the case studies of SSWs are discussed, is rewritten. We extended the general introduction of previous works to a more detailed discussion. Orsolini et al. (2010) is cited and placed in the third paragraph in introduction together with related studies of Manney et al. (2008, 2009).

Lahoz et al. (2011) is cited in **Section 2 (L. 199-201) on the bottom of Page 6**, which is highly related to eddy heat flux in Figure 2. Manney et al. (2009); Lahoz et al. (2011) used tracer isopleths to estimate the descent rate during 2009 SSW. In the CLaMS simulation, $\dot{\theta}$ estimated by diabatic heating is employed as vertical velocity. Using $\dot{\theta}$ in polar region (see Figure 2 d), the descent rate was found to be consistent with the previous studies (Manney et al., 2009; Lahoz et al., 2011) in the sense that 1) the descent rate in the upper stratosphere was much higher than that in the lower stratosphere; 2) the descent rates were the highest in the time period during and shortly after the MW.

- *A smaller point is that I would encourage the authors to use the much more standard acronym “SSW” for “sudden stratospheric warming” (which is in turn preferred to “stratospheric sudden warming” for historical as well as other reasons, e.g., Butler et al, 2015, BAMS) rather than “MW”, which is rather jarring to the reader who is familiar with past SSW studies.*

We replaced the “stratospheric sudden warming” with “sudden stratospheric warming” following the recommendation of Butler et al. (2015). We have considered to replace MW with SSW because, as the reviewer said, some reader may be more familiar with “SSW” than with “MW”. However, because the major sudden stratospheric warming is more standard and precise term here than SSW. Therefore, we now use “major SSW” instead of the abbreviation “MW” throughout the manuscript. We explained it at the beginning of the paper and use this abbreviation consistently.

- *Finally, there are errors in English grammar and usage throughout the paper that render it even more difficult to understand. These are too numerous to note here, but two areas that are consistently problematic are the misuse of commas and the misuse of “which” versus “that” throughout the text. I appreciate the difficulty in writing in a language that is not*

one's native one, and strongly suggest that the authors take advantage of the available editing for English usage before final publication.

We have submitted the revised manuscript to the English proofread department of our research center. However, the proofread costs about 2-3 weeks which will be beyond the deadline of submitting the responses. Thus, we decided to submit the response and manuscript first. The language check will be finished in next few weeks and we will included all the changes in the final publication.

Specific comments

- *Page 4385, lines 6 through 14, these processes (as well as the difficulties that models have in representing them) are not specific to major SSWs. See, e.g., Sutton, et al, 1994, JAS, Fairlie et al, 1997, JGR, Manney et al, 1998, JGR; and references therein.*

We agree that such difficulties are not specific to SSWs. The second paragraph of introduction has been rewritten.

See [the second paragraph on Page 2](#).

- *Page 4385, line 19, Manney et al (2005) and the Manney et al (2008) paper cited here do not discuss composition, except in the context of describing meteorological conditions that affect composition. A second Manney et al (2009) paper - in ACP - does discuss the evolution of MLS-observed trace gases from the UTLS through the lower mesosphere during the 2006 SSW. Manney et al (2009, GRL) discuss composition from the UTLS through the lower mesosphere during the 2009 SSW, not just in the lower stratosphere.*

The third paragraph of introduction has been rewritten.

See [the third paragraph on Page 2](#).

- *Page 4388, lines 4-10, It would be good to cite Butler et al (2014, BAMS) regarding the "standard" definition of a major SSW. Also, the discussion here implies that maximum polar cap temperature is more relevant than the standard diagnostic of circulation reversal (zonal mean 10hPa winds changing sign poleward of 60N) for determining the central day of an SSW - if this is the case, why?*

We are aware that there are different definitions of major SSW as discussed in *Butler et al. (2015)*. Since different criteria introduce no difference in identifying this 08/09 event, the popular criteria (60°N zonal-mean zonal wind on 10 hPa) is used to identify the MW in our study (*Charlton and Polvani, 2007*). Only some small shifts of the onset date can be found by using different criteria and different dataset. Here we cited 2 studies (*Taguchi, 2011; Gómez-Escobar et al., 2014*) which pointed out using the highest polar cap temperature date as the onset date. According to these studies, the response of the BDC to the MW event is better characterized.

See [L.145- 151 on Page 5](#).

- *Page 4388, line 11, and Figure 1 caption, please say what dataset the fields shown in Figure 1 are from.*

Figure 2 (original Figure 1) is based on ERA-interim reanalysis and this information is added in text and figure caption.

See [L. 152- 153 on Page 5](#) and [Figure 2 caption](#).

- *Section 2 overall: The dynamical evolution discussed here should be related to previous work on the dynamics during the 2009 SSW, including (but not limited to) Manney et al (2009, GRL), Labizke and Kunze, 2009, JGR, Ayaraguena et al, 2011, JGR. These papers are cited herein, but the consistency of their results with those shown here is not discussed.*

We agree. To keep connection with previous studies, we added some text in section of dynamical background.

1) Ayaraguena et al. (2011); Harada et al. (2010) studied the planetary wave propagation and its troposphere forcing, which agrees with our E-P flux analysis. We added the statement at [L.183-184 on Page 6](#); 2) The estimation of descent rate studied by Manney et al. (2009); Lahoz et al. (2011) was cited at [L.200-201 on Page 6 in the last paragraph of this section](#) when we discussed the enhanced polar descent based on $\dot{\theta}$.

- *Page 4389, lines 22-23, (a) reference(s) should be given for the wave-driving of the Brewer-Dobson Circulation.*

We added a citation here (Holton et al., 1995).

See [L. 190-191 on Page 6](#).

- *Page 4390, lines 1-9, Hitchcock and Shepherd (2013, JAS) should be included and discussed in relation to radiative timescales during and following SSWs. (In fact, Hitchcock et al, 2013, J Clim, would also be a very good reference to include regarding the vertical structure of dynamical fields during/after SSWs; these papers include discussion of the 2009 event.)*

Hitchcock and Shepherd (2013) is a nice citation here (thanks a lot). We discussed and cited this study.

See [L.205-208 on Page 7](#).

- *Page 4390, line 25, 2500K is not “near the stratopause” in the polar regions immediately following strong, prolonged SSWs, including the 2009 event (e.g., Siskind et al, 2007, GRL, Manney et al, 2008, JGR, France et al, 2012, JGR; and references therein).*

We agree that the stratopause broke down and reformed at a higher altitude (75km) during and after the Major SSW. Our statement is not accurate in this sense. 2500 K is the typical stratopause in boreal winter. Therefore, we changed it to “climatological position of the stratopause”.

See [L. 224 on Page 7](#).

- *Page 4391, lines 6-8, what coordinate is used in the troposphere and how are the vertical velocities determined there?*

The model transforms from the isentropic to the hybrid-pressure coordinate below $\sigma=0.3$ hPa according to the procedure described in *Mahowald et al.* (2002). Thus, the ECMWF ω -velocity is used in the troposphere, which takes into account the effect of large-scale convective transport as implemented in the vertical wind of the meteorological analysis. We avoid this information because the θ coordinate is used in the altitudes we concerned. Nevertheless, we add additional sentence in the manuscript and related citations. See [L. 230-234 on Page 7](#).

- *Page 4391, lines 21-23, presumably the intended meaning is that the simulations with full chemistry and mixing are the reference for the best representation of the atmosphere?*

Yes. For better understanding, we add this statement at [L. 247-248 on Page 8](#).

- *Page 4391, lines 26-27, the vertical coverage of MLS data depends on the species. N₂O is useful only from 100hPa through 0.46hPa, and at pressures of about 5hPa and lower has precision greater than 100%, implying that extensive averaging is needed. The description of “from the troposphere to the mesosphere” is thus not accurate. (In fact, even ozone is only available from the *upper* troposphere.)*

We agree. The description “from the troposphere to the mesosphere” is removed.

- *Page 4391, lines 18-19, I see a small, persistent bias between CLaMS and MLS, with CLaMS O₃ being higher at a given N₂O in Figure 2. Can you say something about the reasons for this bias?*

Looking into the daily validation of CLaMS with MLS on different altitude ranges, the worse correlations (mainly over-estimated ozone of CLaMS) occur at 650 K- 1000 K in mid-latitudes from mid-February to March. We included this sentence into our manuscript. Here we can only speculate the the reason for the differences is a combination of 3 effects: not enough NO_x chemistry or too much ozone production or too fast poleward transport from the tropics (we did not include this statement in the manuscript).

- *Page 4392, lines 23-24, please elucidate what you mean by “very stable”, and to what altitude range this description applies. The vortex on 9 January was, indeed, rather symmetric in the middle and lower stratosphere, but quite elongated and shifted off the pole in the upper stratosphere, and examination of the preceding days shows large variability in shape/position throughout the stratosphere.*

We agree.

See [L. 277 on Page 9](#).

- *Page 4393, line 18, please define “overworld”.*

”Overworld” is not appropriate here, so it was removed.

- *Page 4393, lines 19-21, the description of Nash’s method of defining the vortex edge does not seem quite accurate. Nash defines the vortex edge location as the maximum PV gradient with respect to equivalent latitude, provided that that gradient occurs near enough the wind-speed maximum.*

We agree. The text about Nash’s definition of vortex edge was modified.
See [L. 300-303 on Page 9](#).

- *Page 4394, line 4, please define what you mean by “eddy mixing” here; what other type of mixing are you distinguishing it from?*

We replaced the term “barrier for eddy mixing” by “barrier for propagation of planetary waves”. That is what we wanted to say at this place. Mixing is understood in this paper as a process changing the content of the air parcels, typically with a clear signature in the respective tracer-tracer space (if two air parcels having the same composition do mix, we also call this process mixing, although there is no practical way to detect it). We never use the term “eddy mixing” in this paper. Eddy mixing (i.e. mixing with a strong turbulence created by eddies) leads in most cases to a “true” physical mixing. However, especially within the Lagrangian school, pure trajectories describing chaotic advection are often denoted as eddy mixing.

- *Page 4398, line 4 through Page 4399, line 2: This is one place where clarification of the effects of different processes on the tracer correlations is critical. The intention of the schematic to elucidate that is good, but the discussion is extremely difficult to follow, and did not convey to me how one could use different patterns to diagnose different processes. Further, the effects of chemistry and how they may differ from or mimic transport processes are not represented in this schematic.*

To achieve a better translation between physical space and tracer correlation space, Figure 1 has been added to the introduction in order to provide the basic concept of the tracer- tracer correlations and an overview of dynamics and chemistry impact on the tracer- tracer correlations. We hope this plot can prepare the readers for the upcoming intense discussion on the tracer- tracer correlations in section 5. Moreover, Figure 8 in section 5 has been extended. In particular, physical space interpretations are added to the corresponding tracer correlation patterns. The associated text was also modified. The effect of chemistry is still not discussed in this schematic cartoon.

- *Page 4399, lines 23-27, this is another place where the statements made are not clear to me from the figure.*

Hopefully the new version of section 5 will help.

- *Page 4400, lines 14-15, is there some particular significance (e.g., processes of particular interest) to the focus region chosen in the boxes?*

We explained now in the text, that this choice should help to understand the difference between CLaMS results with and without mixing. We tried to address this point more clearly in [section 5.3.2](#).

- *Page 4400, overall: One of the pervasive difficulties in interpreting tracer correlations is that their morphology depends on non-local effects, and thus by taking very limited latitude or altitude regions, one may be biasing the picture - this discussion seems to me like it may point to such a difficulty?*

Here, once again, we hope that the almost completely rewritten version of section 5 will help.

- *Page 4401, line 22, it is not clear to me what feature in the figure you are describing as a "weak polar correlation"?*

What we mean is “the weak polar correlation resolved with CLaMS (see Fig. 9(c2)) that is not resolved in the MLS observations”, which pointing to the polar correlation shown on Fig. 9(c2) but not in Fig. 9(c1)

See [L. 524-525 on Page 16](#).

- *Section 5.3: The chemical processes discussed here are primarily the gas-phase processes in the middle to upper stratosphere. While tracer correlations have been used extensively (albeit often inaccurately) to examine lower stratospheric polar ozone loss, the impact of the gas-phase chemistry at higher altitudes on them has not been much discussed - therefore, a fuller description of the expected change in tracer correlations in relation to these processes would be helpful. Also, some current and previous studies (e.g., Kuttippurath et al, 2010, ACP, Manney et al, 2015, ACPD) have shown calculations suggesting a small but significant amount of lower stratospheric (chlorine-catalyzed) ozone loss in Dec/Jan 2009 - is this consistent with the suggestion given here that such lower stratospheric loss was negligible?*

We didn't address the chlorine driven polar ozone loss during this winter because *Kuttippurath and Nikulin (2012)* (details see the Fig. 7 in the paper) estimated total ozone column loss in 2008/09 is less than other years without a MW and we also didn't find a persistent and significant polar ozone loss from January to March. However, after reading this paper (*Manney et al., 2015*), we looked back to the period before the MW and did see a small but clear (chlorine-catalyzed) polar ozone loss in lower stratosphere before mid- January due to the unusual low temperature in 2008 early winter (see Fig. 11 b), which is consistent with the SSW case in 2012/13 according to *Manney et al. (2015)*. Therefore, we agree that, similar as 2012/13 early winter with a very cold North pole, the lower stratospheric (chlorine-catalyzed) polar ozone loss in Dec/Jan 2009 is not negligible. We did some changes in the statement. See changes in [L. 61-64 in the introduction and the 2nd paragraph in the section 5.4](#).

- *Page 4406, lines 17-23, is this discussion based on CLaMS, the MLS data, or both?*

The discussion is based on both, Or rather, based on the typical situation of N₂O and O₃ profiles during boreal winter and during the SSW period.

- *Figure 3 caption: state how the vortex edge is defined in the caption.*

Statement is added in the caption.

- *Figure 4, typo “voetex”.*

Changed.

- *Figures 5 and 6, state what the letters represent in the caption. Also, from the discussion in the text, it was unclear whether the letters/numbers used in Figure 5 were or were not related to the same letters/numbers used in Figure 6.*

A sentence was added to the caption.

- *Figure 7, describe in the caption what the black lines represent.*

The statement is added in the caption.

- *Figure 9, say in the caption what the boxes represent.*

The information is added in the caption of Figure 9.

- *Figure 11, say in the caption what the letters A and B in the middle panel represent.*

The information is added in the caption of Figure 11.

- *Figure 13, it would be more intuitive to show the results without the averaging kernel smoothing on the left, and the smoothed fields on the right.*

The layout of Figure 13 has been changed.

References

- Ayarzagüena, B., U. Langematz, and E. Serrano (2011), Tropospheric forcing of the stratosphere: A comparative study of the two different major stratospheric warmings in 2009 and 2010, *Journal of Geophysical Research: Atmospheres (1984–2012)*, 116(D18).
- Butler, A. H., D. J. Seidel, S. C. Hardiman, N. Butchart, T. Birner, and A. Match (2015), Defining sudden stratospheric warmings, *Bulletin of the American Meteorological Society*, (2015), doi: 0.1175/BAMS-D-13-00173.1.

- Charlton, A. J., and L. M. Polvani (2007), A new look at stratospheric sudden warmings. part i: Climatology and modeling benchmarks, *Journal of Climate*, 20(3), 449–469.
- Gómez-Escolar, M., N. Calvo, D. Barriopedro, and S. Fueglistaler (2014), Tropical response to stratospheric sudden warmings and its modulation by the QBO, *Journal of Geophysical Research: Atmospheres*, doi:10.1002/2013JD020560.
- Harada, Y., A. Goto, H. Hasegawa, N. Fujikawa, H. Naoe, and T. Hirooka (2010), A major stratospheric sudden warming event in january 2009, *Journal of the Atmospheric Sciences*, 67(6), 2052–2069.
- Hegglin, M. I., and T. G. Shepherd (2007), O₃-n₂o correlations from the Atmospheric Chemistry Experiment: Revisiting a diagnostic of transport and chemistry in the stratosphere, *J. Geophys. Res.*, D19301, doi:10.1029/2006JD008281.
- Hitchcock, P., and T. G. Shepherd (2013), Zonal-mean dynamics of extended recoveries from stratospheric sudden warmings, *Journal of the Atmospheric Sciences*, 70(2), 688–707.
- Holton, J. R., P. Haynes, M. E. McIntyre, A. R. Douglass, R. B. Rood, and L. Pfister (1995), Stratosphere-troposphere exchange, *Rev. Geophys.*, 33, 403–439.
- Kuttippurath, J., and G. Nikulin (2012), A comparative study of the major sudden stratospheric warmings in the arctic winters 2003/2004–2009/2010, *Atmospheric Chemistry and Physics*, 12(17), 8115–8129.
- Lahoz, W., Q. Errera, S. Viscardy, and G. Manney (2011), The 2009 stratospheric major warming described from synergistic use of BASCOE water vapour analyses and MLS observations, *Atmospheric Chemistry and Physics*, 11(10), 4689–4703.
- Mahowald, N. M., R. A. Plumb, P. J. Rasch, J. del Corral, and F. Sassi (2002), Stratospheric transport in a three-dimensional isentropic coordinate model, *J. Geophys. Res.*, 107(D15), 4254, doi:10.1029/2001JD001313.
- Manney, G. L., M. J. Schwartz, K. Krüger, M. L. Santee, S. Pawson, J. N. Lee, W. H. Daffer, R. A. Fuller, and N. J. Livesey (2009), Aura microwave limb sounder observations of dynamics and transport during the record-breaking 2009 arctic stratospheric major warming, *Geophysical Research Letters*, 36(12), L12,815, doi:10.1029/2009GL038586.
- Manney, G. L., Z. Lawrence, M. Santee, N. Livesey, A. Lambert, and M. Pitts (2015), Polar processing in a split vortex: Arctic ozone loss in early winter 2012/2013, *Atmospheric Chemistry and Physics*, 15(10), 5381–5403.
- Manney, G. L., et al. (2008), The evolution of the stratopause during the 2006 major warming: Satellite data and assimilated meteorological analyses, *Journal of Geophysical Research: Atmospheres (1984–2012)*, 113(D11), doi:10.1029/2007JD009097.
- Michelsen, H. A., G. L. Manney, M. R. Gunson, and R. Zander (1998), Correlations of stratospheric abundances of NO_y, O₃, N₂O, and CH₄ derived from ATMOS measurements, *J. Geophys. Res.*, 103, 28,347–28,359.

- Orsolini, Y. J., J. Urban, D. P. Murtagh, S. Lossow, and V. Limpasuvan (2010), Descent from the polar mesosphere and anomalously high stratopause observed in 8 years of water vapor and temperature satellite observations by the odin sub-millimeter radiometer, *J. Geophys. Res.*, *115*(D12).
- Plumb, R. A. (2007), Tracer interrelationships in the stratosphere, *Rev. Geophys.*, *45*, RG4005, doi:10.1029/2005RG000179.
- Ray, E. A., F. L. Moore, J. W. Elkins, D. F. Hurst, P. A. Romashkin, G. S. Dutton, and D. W. Fahey (2002), Descent and mixing in the 1999-2000 northern polar vortex inferred from in situ tracer measurements, *J. Geophys. Res.*, *107*, 8285, doi:10.1029/2001JD000961.
- Sankey, D., and T. G. Shepherd (2003), Correlations of long-lived chemical species in a middle atmosphere general circulation model, *J. Geophys. Res.*, *108*(D16), 4494, doi: 10.1029/2002JD002799.
- Taguchi, M. (2011), Latitudinal extension of cooling and upwelling signals associated with stratospheric sudden warmings, *Journal of the Meteorological Society of Japan. Ser. II*, *89*(5), 571–580.

Impact of the 2009 major sudden stratospheric warming on the composition of the stratosphere

Mengchu Tao¹, Paul Konopka¹, Felix Ploeger¹, Jens-Uwe Grooß¹, Rolf Müller¹, C. Michael Volk², Kaley A. Walker³, and Martin Riese¹

¹Forschungszentrum Jülich (IEK-7: Stratosphere), Germany

²Department of Physics, University of Wuppertal, Germany

³Department of Physics, University of Toronto, Toronto, Ontario, Canada

Correspondence to: M. Tao (m.tao@fz-juelich.de)

Abstract. In a case study of a remarkable major Sudden Stratospheric Warming (SSW) during the boreal winter 2008/09, we investigate how transport and mixing triggered by this event affect the composition of the entire stratosphere in the northern hemisphere. We simulate this event with the Chemical Lagrangian Model of the Stratosphere (CLaMS), both with optimized mixing parameters and with no mixing, i.e. with transport occurring only along the Lagrangian trajectories. The results are investigated by using **tracer-tracer correlations** and by applying the Transformed Eulerian Mean formalism. The CLaMS simulation of N₂O and O₃ and in particular of the O₃-N₂O tracer correlations with optimized mixing parameters shows good agreement with the Aura Microwave Limb Sounder (MLS) data. The spatial distribution of mixing intensity in CLaMS correlates fairly well with the Eliassen-Palm flux convergence. This correlation illustrates how planetary waves drive mixing. By comparing simulations with and without mixing, we find that after the SSW poleward transport of air increases not only across the vortex edge but also across the subtropical transport barrier. Moreover, the SSW event, at the same time, accelerates polar descent and tropical ascent of the Brewer-Dobson circulation. The accelerated ascent in the tropics and descent at high latitudes first occurs in the upper stratosphere and then propagates downward to the lower stratosphere. This downward propagation takes over one month from the potential temperature level of 1000 K to 400 K.

1 Introduction

A major Sudden Stratospheric Warming (major SSW) is a dramatic phenomenon with strong wind disturbance and polar temperature rise in the winter stratosphere, associated with transport of air

from low to high latitudes (see e.g. Andrews et al., 1987). The mechanism of SSWs has been understood as a result of tropospheric waves propagating upwards into the stratosphere and breaking at a certain level (Matsuno, 1971). Planetary-scale waves can be diagnosed by the Eliassen-Palm (EP) flux and its divergence (Eliassen, 1951; Plumb and Bell, 1982). In particular, positive and negative values of the EP flux divergence quantify the acceleration and deceleration of the westerly zonal flow, respectively, driving the Brewer-Dobson (BD) circulation (e.g., Holton et al., 1995).

Resolving filamentary structures explicitly and realistically representing the dissipation/mixing processes in models is important for simulating non-linear chemical reactions accurately (Tuck, 1986; Orsolini et al., 1997; Edouard et al., 1996; Konopka et al., 2003). However, resolving these structures accurately is a general difficulty for chemical transport models (e.g., Sutton et al., 1994; Fairlie et al., 1997; Manney et al., 1998). During a SSW event, strong large-scale planetary waves propagate, break and finally dissipate – a process that occurs almost isentropically, i.e. on levels with a constant potential temperature. In the stratospheric chemical tracer fields, the SSW itself is characterized by the existence of filamentary structures on a broad range of spatial scales (see e.g. McIntyre and Palmer, 1983; Konopka et al., 2003, 2005; Groöß et al., 2005). Therefore, quantitative understanding of SSWs is a challenge for current chemical transport models in particular in terms of coupling between dynamics, transport and chemistry.

To improve the understanding of SSWs, many case studies based on reanalysis data, modeling and/or satellite data have been performed. Manney et al. (2005, 2008) described the synoptic evolution during the 2004 and 2006 Sudden Stratospheric Warmings (SSW). Based on the Aura Microwave Limb Sounder (MLS) observations, the meteorology and trace gases from the UTLS to the lower mesosphere during 2006 and 2009 SSW were extensively studied (Manney et al., 2009a, b). Using satellite temperature measurements during three major SSWs, an anomalously strong descent of mesospheric air into the upper stratosphere was found along with the stratopause breaking and then reforming above 75 km (Manney et al., 2008, 2009b; Orsolini et al., 2010). The major SSW in 2009 was the most intensive and prolonged case in the record (Manney et al., 2009b) and this event happened although typical known external factors, e.g. the Quasi-Biennial Oscillation, the Southern Oscillation, the 11-year sunspot cycle, were all unfavorable for the occurrence of a SSW (Labitzke and Kunze, 2009). Ayarzagüena et al. (2011) and Harada et al. (2010) studied this event from the perspective of tropospheric forcing. Both studies pointed out that the pronounced planetary wave-2 in the stratosphere, which triggers the SSW, is associated with a high-pressure ridge over the Pacific.

The remarkable stratospheric warming event in 2009 strongly influenced the distribution of chemical species. The amount of air transported out of the polar vortex into the mid-latitudes was weakest before the major SSW and strongest after this event (Manney et al., 2009b). Kuttippurath and Nikulin (2012) diagnosed an increasing trend of occurrence of NH major SSWs in recent years (1999–2011). They confirmed a weakening in the chlorine-induced ozone loss after the onset of major SSWs dur-

ing 2003/04, 2005/06 and 2008/09 winters. Sofieva et al. (2012) used Global Ozone Monitoring by Occultation of Stars (GOMOS) satellite measurements to study the O₃, NO₂ and NO₃ distribution during the **three major SSWs** and found that changes in chemical composition due to major SSWs can extend into the mesosphere and even into the lower thermosphere. **Manney et al. (2015) studied the 2012/13 winter and pointed out that, although the chlorine-induced ozone loss became weak after the onset of SSW, the ozone loss was significant due to the unusual low temperature in the lower stratospheric polar vortex before the SSW (mainly in December and January).**

65 From the Lagrangian perspective, atmospheric transport can be divided into advection, which describes transport of an air parcel along a 3D trajectory, and mixing, which makes the representation of transport barriers in Eulerian models difficult (Sankey and Shepherd, 2003; Hegglin and Shepherd, 2007; Hoppe et al., 2014). Compared to Eulerian transport models with an implicit numerical diffusion, Lagrangian transport models have advantages in separating mixing from advection and thus explicitly describe the mixing process in the atmosphere. Here, we use the Chemical Lagrangian Model of the Stratosphere (CLaMS), which is based on Lagrangian transport and parametrized mixing along the trajectory by adaptive re-gridding after every 24 hours time step (McKenna et al., 2002b). The mixing parametrized small-scale mixing in CLaMS is induced by large-scale flow deformations, e.g. by wave breaking (Konopka et al., 2004, 2007). Advection in CLaMS is driven by the European Centre for Medium-range Weather Forecasts (ECMWF) ERA-Interim reanalysis horizontal winds and **cross isentropic vertical transport is deduced from diabatic heating rates** (Dee et al., 75 2011; Ploeger et al., 2010).

An appropriate representation of mixing in the models is the main difficulty for an accurate description of the permeability of transport barriers like the polar vortex edge or the tropical pipe (Tuck, 80 1986; Plumb, 1996; Steinhilber et al., 2005; Hoppe et al., 2014). Mixing itself is an irreversible process which, in a stably stratified stratosphere, is mainly driven by isentropic stirring that is associated with large-scale wave breaking and wind shear (McIntyre and Palmer, 1983). Riese et al. (2012) assessed the influence of uncertainties in the atmospheric mixing strength on the global distribution of the greenhouse gases H₂O, O₃, CH₄ and N₂O in the upper troposphere and lower stratosphere (UTLS) and on the associated radiative effects. Their results show that simulated radiative effects of H₂O and O₃, both characterized by steep gradients in the UTLS, are particularly sensitive to the atmospheric mixing strength. 85

To separate and quantify the impact of mixing on transport and chemistry of stratospheric constituents during a SSW, we utilize tracer-tracer correlations. Chemical constituents in the stratosphere whose chemical sources and sinks are slow compared with dynamical timescales, are influenced by the Brewer-Dobson circulation and by quasi-isentropic mixing (which is most efficient within the extratropical surf zone) and show compact tracer-tracer relations (Plumb, 2007). Mixing is suppressed at the edge of the winter polar vortex and at the edges of the tropics, so that tracer relationships distinct from those of middle latitudes occur in the tropics and in the polar vortices (e.g., Plumb, 90

95 1996; Volk et al., 1996; Müller et al., 1996, 2001; Plumb, 2007). Here, we focus on the relationship
of O_3 with the long-lived tracer N_2O . Because chemical production and loss terms of O_3 increase
strongly with altitude in the stratosphere, ozone can not be considered long-lived at altitudes above
 ≈ 20 km and relations with N_2O are not necessarily compact (Hegglin and Shepherd, 2007). **Con-**
ditions are different in the polar vortex in winter, where the lifetime of ozone exceeds half a year
100 **(Sankey and Shepherd, 2003)**. However, the transport barriers in the stratosphere are sufficiently
strong to allow distinct tracer-tracer relationships, in particular different O_3 - N_2O relationships to
develop in the polar vortex, the mid latitudes and in the tropics (Michelsen et al., 1998; Ray et al.,
2002; Müller et al., 2005; Hegglin and Shepherd, 2007).

Because different O_3 - N_2O relationships prevail in the polar vortex, in mid-latitudes and in the
105 tropics, mixing of air masses from these different regions will change O_3 - N_2O relationships, even
if relations in a particular region are linear (Fig. 1, top panel). Mixing between the polar vortex
and mid-latitudes and between mid-latitudes and the tropics occurs along quasi-isentropic surfaces
(Proffitt et al., 1990; Müller et al., 2005). Because the location of the isentropes in O_3 - N_2O space,
mixing of mid-latitude and polar air will lead to higher ozone and higher N_2O in the polar region
110 and mixing of mid-latitude and tropical air will lead to lower N_2O and lower ozone in the tropics
(Fig. 1, top panel). The effect of mixing between polar and mid-latitude air on O_3 - N_2O relationships
and the occurrences of this process along quasi-isentropic surfaces is also clearly visible (albeit
likely in an exaggerated way) in model simulations (Sankey and Shepherd, 2003; Müller et al., 2005;
Lemmen et al., 2006).

115 Upwelling and downwelling of stratospheric air changes tracer mixing ratios at a particular al-
titude (or potential temperature level) but does *not* change the tracer-tracer correlation (Ray et al.,
2002). Therefore O_3 - N_2O relationships will not be affected by up- and downwelling (Fig. 1, mid-
dle panel), while however the location of the potential temperature surfaces in O_3 - N_2O space will
change. Because of the vertical profile of ozone and N_2O below altitudes of ≈ 700 K, downwelling
120 in the polar region will lead to an upward bending (more ozone, less N_2O) of the isentropes, while
upwelling in the tropics will lead to downward bending (less ozone, more N_2O) of the isentropes
(Fig. 1, middle panel, grey lines).

Finally, chemistry will impact O_3 - N_2O relationships; indeed ozone-tracer relations have been
used extensively to examine lower stratospheric ozone loss in the polar regions (e.g., Proffitt et al.,
125 1990; Müller et al., 1996, 2001; Tilmes et al., 2006). On the timescales and for the altitudes of in-
terest here, only chemical change for ozone needs to be taken into account. Thus, chemical loss of
ozone in the polar regions shifts the O_3 - N_2O relationship downward, towards lower ozone mixing
ratios and chemical production of ozone in the tropics will shift the O_3 - N_2O relationship upwards
towards higher ozone mixing ratios (solid and dashed black lines in Fig. 1, bottom panel). In a model
130 simulation the impact of chemistry on ozone-tracer relations can be investigated further through sim-
ulations using passive (i.e., chemically inert) ozone; this point will be discussed below in section 5.

The motivation of this work is to improve our understanding of transport and its impact on chemistry in a stratosphere under strongly disturbed dynamical conditions. In particular, the 2009 major SSW is an excellent case for studying: 1) the multi-timescale (days to months) responses to the wave forcing; 2) the evolution of mixing and its effect on distribution of chemical composition; 3) the observed tracer-tracer correlations using CLaMS simulations. In section 2, we will present an overview of the dynamical background of the stratospheric winter 2008/09. The CLaMS setup and validation of CLaMS result with the MLS observations of N_2O and O_3 will be presented in section 3. Section 4 will discuss the simulated mixing intensity in relation to wave forcing. Finally, section 5 will present the N_2O - O_3 correlations and their interpretation in terms of mixing, advection and chemistry caused by the major SSW in January 2009. Finally, the main results will be concluded in section 6.

2 Dynamical background

The definitions for SSW and classifications are extensively discussed by Butler et al. (2015). According to commonly used criteria (Christiansen, 2001; Charlton and Polvani, 2007), we identify the warming event on January 24th by the reversal of $60^\circ N$ westerly zonal-mean wind at 10 hPa. As has been pointed out (Taguchi, 2011; Gómez-Escolar et al., 2014), use of the highest polar cap temperature instead of the zonal wind reversal at $60^\circ N$ and 10 hPa, characterizes the response of the BDC to SSWs better. Thus, we use January 23rd as the central day of SSW because the polar cap temperature reached its peak on January 23rd.

Figure 2 gives an overview of the dynamical background during the boreal winter 2008/09 based on ERA-Interim reanalysis. Fig. 2a shows that the sudden rise of the polar cap temperature started in the upper stratosphere, around January 10th at 1 hPa. Thereafter, the warming propagated downward, arriving at 10 hPa and descended to the lower stratosphere until late January. The increase of polar temperature was accompanied by the generation of easterlies, which are also shown in Fig. 2a (black contours). The rise in easterlies and temperature lasted only 10 days at 1 hPa followed by a strong polar vortex cooling while the disturbance of wind and temperature in the lower stratosphere lasted more than 1 month without a complete recovery until the final warming in the spring of 2009.

Before the major SSW, the lower stratosphere in the tropics was slightly warmer than the long-term average due to the westerly phase of the QBO in this winter. Similar to the warming in the high latitudes, the tropical cooling (Fig. 2b) also started at about January 15th at 1 hPa and descended from the upper to the lower stratosphere over 2 weeks. As discussed in Randel et al. (2002), time-dependent upwelling in the tropical lower stratosphere is correlated with transient extratropical planetary waves, which transport heat from the tropics to high latitudes and, in turn, drive the BD-circulation.

A widely used diagnostic of the upward-propagating planetary waves is the vertical component of the EP flux, for which the strongest contribution results from the horizontal eddy heat flux $\overline{v'T'}$ with $v' = v - \bar{v}$, $T' = T - \bar{T}$ and with overbar denoting zonal mean and primes describing the deviations (i.e. fluctuations) for the temperature T and for the meridional velocity v (Andrews et al., 170 1987; Newman et al., 2001). Fig. 2(e) shows the time evolution of the eddy heat flux at 100 hPa averaged between 40 and 70°N, which explains more than 80% of the variability of the total vertical component of the EP flux. In addition, contributions of the wave-1 and wave-2 components to the mean eddy heat flux are also shown.

Newman et al. (2001) pointed out that the eddy heat flux measures activity of the waves and is 175 highly correlated with the time evolution of the stratospheric polar temperature. As can be deduced from Fig. 2e and Fig. 2a (or Fig. 2b), the mean eddy heat flux at 100 hPa was well correlated with warming at the North Pole and cooling in the tropics. It shows a 1~2 weeks oscillation ranging within 0-25 K m s^{-1} in December and it began to increase from January 6th reaching the first peak on January 18th. After several days of a slight decay, it rose up to the second peak on January 27th 180 and then gradually declined to zero around mid-February with some small fluctuations afterwards. The dominant wave number before and during the major SSW was wave-2 that led to the vortex split. **The dominant and extraordinary planetary wave-2 is associated with unusual development of the upper tropospheric ridge over Alaska (Ayarzagüena et al., 2011; Harada et al., 2010).** However, after the major SSW, the main contribution to the total eddy heat flux resulted from higher wave 185 numbers.

Large-scale tropospheric waves can propagate upward into the stratosphere through weak west-erlies and break at the critical level, disturbing the mean flow (Dickinson, 1968; Matsuno, 1971). **Such a transient wave breaking converts the zonal flow momentum to mean meridional circulation, and thus drives the extra-tropical downwelling and tropical upwelling of the BD circulation** 190 **(e.g., Holton et al., 1995).** The temperature perturbations discussed above and shown in Fig. 2 (a,b) result directly from diabatic heating and cooling caused by these wave-driven vertical motions. Subsequently, temperatures gradually relax toward their radiative equilibrium values by additional radiative cooling or heating, causing vertical motion, i.e. down- or upwelling through isentropic surfaces. The polar and tropical (total) diabatic heating rate anomalies from the 24-year mean of ECMWF 195 meteorological ERA-Interim reanalysis (Dee et al., 2011) are shown in Fig. 2 (d,e). As expected, diabatic polar downwelling and tropical upwelling (quantified by these heating rates) were both accelerated after the onset of the major SSW. **The polar vortex descent rate strongly increased around Jan. 25th up to 15 K/day on 1000 K and only around 3 K/day on 500 K during the late January. The variability of polar vortex descent rate reported here is consistent with the findings by Manney et al.** 200 **(2009b) and Lahoz et al. (2011) where the tracer isopleths method based on MLS observations of N_2O , CO and H_2O was used.** The onset of the heating rate anomalies at each altitude, and thus their downward propagation, is roughly synchronous with the temperature anomalies shown in Fig. 2

(a,b). The radiative decay of the anomalies takes only about 10 days at 1000 K, but more than one month below 500K. This is consistent with the stratospheric radiative relaxation time inferred from satellite measurements (Mlynczak et al., 1999), which was found to increase from 10 days at 1 hPa to about 100 days at 50 hPa. This is also consistent with a strong suppression of planetary wave propagation into the vortex after the major SSW (Hitchcock and Shepherd, 2013).

3 Model description and validation

3.1 Model setup

CLaMS is a Lagrangian chemistry transport model that can be run with or without mixing, so that the whole transport is carried out only along 3d forward trajectories. However, a pure Lagrangian transport approach gives rise to many unrealistic small-scale structures due to lack of mixing (Konopka et al., 2004; Khosrawi et al., 2005). Hence, irreversible small-scale mixing between air parcels (APs) should be considered. With the concept that (small-scale) mixing is driven by large-scale flow deformation, the CLaMS mixing procedure is realized through adaptive re-gridding of the irregular grid. More specifically, the APs are inserted or merged when the distances between the next neighbors increase above or decrease below a critical distance. The critical deformation γ_c is defined as $\gamma_c = \lambda_c \Delta t$, with the critical Lyapunov exponent λ_c and the advective time step Δt set to 1.5 day^{-1} and 24 hours, respectively (for more details see McKenna et al., 2002b; Konopka et al., 2004).

CLaMS simulations cover the 2008/09 boreal winter from December 1st, 2008 to April 1st, 2009 and extend between the Earth's surface and the potential temperature $\theta = 2500 \text{ K}$ (i.e. roughly around the climatological position of the stratopause with $p \approx 0.3 \text{ hPa}$). The horizontal separation of the APs initialized on December 1st is 70 km in the NH, where all our results are obtained, and 200km in the SH. During the course of the simulation, this irregular grid of APs undergoes advection along the trajectories, chemistry and mixing every time step, with $\Delta t = 24 \text{ hours}$ (Konopka et al., 2004; Grooß et al., 2005; Pommrich et al., 2014).

The horizontal winds are prescribed by the ECMWF ERA-Interim reanalysis (Dee et al., 2011). To resolve both transport processes in the troposphere influenced by the orography and in the stratosphere where adiabatic horizontal transport dominates, a hybrid coordinate is used as proposed by Mahowald et al. (2002). In the stratosphere and in the UTLS, potential temperature θ is employed as the vertical coordinate of the model above 300 hPa and the cross-isentropic velocity $\dot{\theta} = Q$ is deduced from the ERA-Interim forecast total diabatic heating rates Q , including the effects of all-sky radiative heating, latent heat release and diffusive heating as described by Ploeger et al. (2010). The time evolution of the anomaly of $\dot{\theta}$ averaged over the polar cap and over the tropics is shown in Fig. 2 (c,d) and was discussed in the previous section.

N₂O and O₃, the most important species **for this work**, are initialized from the MLS data (more details on MLS can be found in the next subsection). The other chemical species are initialized from a multi-annual CLaMS simulation with simplified chemistry (Pommrich et al., 2014) as well as from
240 gridded MLS data of HCl, H₂O and CO. The employed method uses tracer-tracer correlations (for more details see Grooß et al., 2014). At the upper boundary (2500 K) O₃ is set to the HALOE climatology after every 24 hours time step. However, the impact of the upper boundary condition on the chemical tracers is not significant below 1000 K. The chemistry module of CLaMS is described in details in McKenna et al. (2002a).

245 By switching off and on the mixing module, we get two sets of simulations: full chemistry without mixing and full chemistry with mixing. **The simulation with full chemistry and with mixing is the reference as the best model representation of the real atmosphere.** Both simulations include ozone calculated with full chemistry (O₃) and passively transported O₃ without any chemistry (pO₃).

3.2 Validation with the MLS observations

250 MLS observes microwave emission from the limb of the Earth's atmosphere in the direction of the Aura orbit. **The instrument measures vertical profiles** every 165km (1.5° along the Aura orbit), providing about 3500 profiles per day. We use version 3.3 N₂O and O₃ from the MLS product (Livesey et al., 2011) both to initialize and to validate the CLaMS reference simulation. The vertical resolution of O₃ is about 2.5-3 km in the stratosphere with a 5-10% uncertainty (Livesey et al.,
255 2011, 2013). The vertical resolution of N₂O is about 4-6 km with a 9-25% uncertainty for the region of interest in this study (Livesey et al., 2011). Averaging kernels are applied in the retrieval of the MLS profiles, which relate the retrieved MLS profiles to the true atmospheric state. More details about MLS v3.3 measurements, data validation and processing algorithms are available at http://mls.jpl.nasa.gov/data/v3-3_data_quality_document.pdf.

260 For comparison, we map CLaMS mixing ratios to the observed MLS profiles using a back and forward trajectory technique (Ploeger et al., 2013) and apply the MLS averaging kernels to CLaMS output in order to get comparable quantities (see Appendix). Because CLaMS APs are saved every day only at 12 UTC, we calculate the noon-positions of the MLS observations within 1 day window using back and forward trajectories, and then select the nearest CLaMS AP to the corresponding
265 MLS observation. The mixing ratios at this AP are then compared with the respective MLS observations.

Hereby, a one-to-one MLS-CLaMS data set for N₂O and O₃ is established that is plotted in Fig. 3 as probability distribution functions (PDFs) calculated for the whole NH and for the entire simulation period (around 10 thousand points). According to a high correlation coefficient both for N₂O
270 (0.957) and for O₃ (0.989), our reference simulation matches the MLS observations fairly well. The largest difference was diagnosed in the θ -range between 650 and 1000 K where CLaMS O₃ slightly overestimates the MLS observations.

For a further comparison, we investigate the horizontal distribution of N_2O . Figure 4 shows the comparison between the CLaMS simulation and MLS observations for five selected days at $\theta = 800$ K (top 2 panels) and 475 K (bottom 2 panels). On January 9th, the vortex was centered around the North Pole and the vortex structure was stable in the middle and lower stratosphere. Mainly influenced by the planetary wave-2, the polar vortex stretched to North America and Asia on both heights during the following days. Around the central day of the major SSW at January 23rd, a double center structure formed which split up until January 25th at 475 K and until January 28th at 475 K (not shown).

In the following days, an increasing number of filaments could be observed outside of the vortex characterized by low N_2O values. The two vortex centers slowly rotated anticlockwise. One of the vortex remnants over eastern North America and the Atlantic stretched further, split and dissolved releasing its content to mid-latitudes, while another one stayed over northern Asia and the Pacific Ocean. Although in the following weeks most of the vortex fragments were mixed with mid-latitude air, a part of them, like those over northern Asia and the Pacific Ocean, re-organized as a new and relatively weak vortex. However, this top-down process that has started in late February at 800 K (a weak, circumpolar vortex edge can be diagnosed at $\theta = 800$ K at February 20th, see Fig. 4) and was finished in mid March at 475 K (not shown) is excluded from our analysis, which ends with February 28th.

The distribution of simulated N_2O accurately represents the MLS observations, although more filamentary structures are resolved in CLaMS simulations than MLS observations. It should be noted that applying averaging kernels to model result also smoothes out some valuable information, e.g. filamentary structures, and, consequently, may result in a misinterpretation of the stratospheric composition, especially for high-latitude N_2O . More details are discussed in the Appendix.

4 Planetary waves and mixing

4.1 Transport and mixing barriers in the winter hemisphere

In the winter stratosphere, there exist two main barriers to transport, shown by the two thick blue lines in Fig. 5 (Holton et al., 1995). One is the polar vortex edge, which can be identified as the maximum gradient of potential vorticity (PV) with respect to equivalent latitude within a certain range where maximum of wind speed along equivalent latitudes (in the following eq. latitude) occurs (Nash et al., 1996). The second barrier (around 10-30°N eq. latitudes, varying with altitude) separates the mid-latitude surf zone (McIntyre and Palmer, 1983) from the region of tropical upwelling, the so-called tropical pipe (Plumb, 1996).

This subtropical barrier is not as well-defined as the polar vortex edge and is usually characterized by a much weaker PV gradient between tropics and mid-latitudes (Polvani et al., 1995) although large meridional tracer gradients can be diagnosed (Shuckburgh et al., 2001; Punge et al., 2009;

Konopka et al., 2010). While the polar vortex edge is considered as a meridional transport barrier due to a strong polar jet, the subtropical barrier is only weakly influenced by the jets and is usually understood as a barrier for **propagation of planetary waves**. This barrier is strongly related to the phase of the Quasi-Biennial Oscillation (QBO): during the westerly QBO, planetary waves generated in the winter hemisphere can propagate across the equator to dissipate at the summer hemisphere **easterlies**, whereas such propagation is suppressed during the easterly QBO phase (Haynes and Shuckburgh, 2000; Shuckburgh et al., 2001; Punge et al., 2009). Thus, during the 2008/09 winter, the subtropical transport barrier was weakened by the westerly QBO phase (dashed thick blue line in Fig. 5).

In a winter with weak activity of planetary waves, the exchange and mixing of air across the vortex edge is suppressed. However, once a sudden warming event happens, the enhanced wave forcing drives significant isentropic, two-way mixing (red curved arrows) as well as the large-scale BD circulation (gray arrows). The evolution of the dynamical fields, including cross-isentropic vertical velocity $\dot{\theta}$ and zonal wind, was discussed in the previous section (Fig. 2). But isentropic mixing and its relation to wave forcing need further investigation.

4.2 CLaMS mixing versus wave forcing

Mixing between the Lagrangian APs is parametrized in CLaMS through adaptive re-gridding. During this process, the involved APs (i.e. APs, which were generated by the mixing algorithm), are marked after every 24 hours time-step. Here we use the statistics of these events, i.e. the percentage of mixed APs relative to all transported APs, in the following denoted as mixing intensity. In this way, we illustrate the impact of the major SSW on the distribution and evolution of mixing resolved by the model.

Figure 6 shows the time evolution of the zonally averaged mixing intensity derived from CLaMS versus eq. latitude. **Fig. 7 illustrates** the relationship between the EP flux divergence and the CLaMS mixing intensity averaged over several stages of the polar vortex during the winter 2008/09: (a) stable **vortex** conditions in January between 3rd and 13th, (b) **10 day period** before the major SSW, i.e. between 14th and 23rd of January, (c) **10 day period** after the major SSW, i.e. between January 24th and February 3rd, and (d) stable stratospheric conditions after the major SSW between 4th and 13th of February.

We notice that before mid January maximum mixing remains equatorward of 65°N and generally outside the polar vortex boundary as defined by the Nash criterion (Fig. 6). In particular above 700 K the rather abrupt poleward decrease in mixing strength clearly marks the polar mixing barrier isolating the core of the stable polar vortex from the surf zone. Note that the Nash criterion is not necessarily a perfect proxy for the mixing barrier, thus mismatch to within a few degrees latitude, as apparent in Fig. 6a. In mid-January the picture changes drastically. With the intensified wave activity disturbing the polar vortex, the westerlies decelerated. Consequently, the EP flux increased and its divergence became strongly negative meaning an enhanced convergence of the EP-flux (Fig. 7).

Furthermore, the pattern of mixing intensity separated into two branches above 700K after Jan. 24th
345 (Fig. 6a): one in high and another one in mid eq. latitudes (marked as A1 and A2 in Fig. 6a and
Fig. 7c, respectively).

This distribution of mixing intensity indicates that both the polar and subtropical barrier (the latter
above 700 K) are weakened by the major SSW. Furthermore, daily PV or tracer distributions over
the NH (cf. Fig. 3) exhibit that at this time several vortex fragments move equatorward and mix with
350 mid-latitude air. At the same time, several fragments of tropical air masses which are generated at
low latitudes, are transported poleward and mixed with mid- or high latitude air.

Mixing intensity diagnosed in Fig. 6 shows some interesting, altitude-dependent patterns: At the
highest levels (θ between 700 and 850 K) **after the major SSW**, the mid- and high-latitude mixing
is comparable (cf. A1 versus A2 in Fig. 6a). At the levels between 500 and 700 K, the high-latitude
355 mixing branch within the vortex dominates. Finally, in the lower stratosphere between 400 K and
500 K, mixing has intensified in the polar region after the major SSW while the mixing intensity
in the surf zone (marked by B in Fig. 6(c)) has slightly increased during and after the major SSW.
Note that the subtropical barrier can be identified as a minimum in mixing intensity between 10°N
and 20°N eq. latitude (Fig. 6b). The position of this minimum does not significantly change during
360 the time **shown** although the impact of the major SSW can be seen around February 1st, mainly at
highest levels between 700 and 850 K.

From the vertical cross sections of EP flux shown in Fig. 7, we infer that in the first half of
January, there were 3 intensive mixing regions (marked as A, B and C) with only weak, vertically
propagating waves. As mentioned above, region A became stronger during the course of the winter
365 and then divided into two branches (A1 and A2). Region B is related to the mid-latitude (surf zone)
mixing in the lower stratosphere (400 - 500 K) that is influenced by the subtropical jet and the QBO.
Region C is associated with strong vertical shear in the transition layer between the westerlies and
easterlies of the QBO.

It is obvious that although before the major SSW high mixing intensities can be diagnosed in the
370 surf zone outside of the polar vortex (region A), this signature intensifies after the onset of the major
SSW (regions A1 and A2). Convergence of the EP flux indicates breaking of waves and thus leads
to wave-mean-flow interaction. Once the local wind field is significantly disturbed by transport of
momentum and heat flux, subsequent stirring and stretching of eddies (resolved by the ECMWF
winds) drives the mixing parametrization in CLaMS. Note that after Feb. 10th (20 days after the
375 SSW), the mixing intensity quickly dropped as the vortex started to recover with a weak vortex edge
between 50 and 60°N eq. latitude at 800 K and 50°N eq. latitude at 600 K (i.e. with a weak PV
gradient according to the Nash criterion).

Based on the analysis of the temporal and spatial evolution of the mixing intensity resolved in
CLaMS and the EP flux divergence, the simulated patterns show a clear and reasonable **physical**
380 **picture how mixing responds** to large-scale wave forcing: when the general circulation is strong and

stable, the mixing pattern is also stable; when the general circulation is disturbed and weakened by the large-scale wave forcing, the pattern of mixing is largely determined by the local wave activities. However, the question still arises whether mixing resolved by the model can also be seen in the observations. **This would help to provide a more quantitative understanding of how the major SSW**
385 influences the chemical composition of the stratosphere.

5 Impact of the major SSW on transport and chemistry

5.1 N₂O-O₃ correlations: MLS versus CLaMS

As discussed in the last section, the subtropical barrier and **even more so** the polar vortex barrier suppress the exchange of air across those barriers before the major SSW. Hence, long-lived species
390 are well-mixed in the regions segregated by these barriers and strong isentropic gradients of these species are expected across such barriers. In **the tracer-tracer space** (in the following abbreviated as tracer space), these well-mixed regions manifest as compact correlations; however correlations between the tracers are different in the regions segregated by barriers (for a review of this method see Plumb, 2007).

395 Figure 9 (a1)-(c1) **show the N₂O-O₃ correlations of MLS observations plotted as probability distribution functions (PDFs)**. The data **cover** the NH with eq. latitudes between 0 and 90°N and within the potential temperature range between 450 and 700 K. The MLS observations are selected for three periods: December, 18-28th (one month before the major SSW), January, 18-28th (during the major SSW); February, 18-28th (one month after the major SSW). The gray lines in Fig. 9(a1)-(c1)
400 indicate the isentropes calculated from the pressure altitude of the observations and corresponding ECMWF temperature.

Under relatively stable dynamical conditions before the major SSW, **two stronger and one weaker branches of N₂O-O₃ correlations** with enhanced PDF values can be distinguished in Fig. 9(a1). **These branches describe the well-mixed air masses within the polar vortex, the surf zone and the**
405 **tropics** (thin black lines from bottom to the top, respectively). The corresponding barriers in the physical space, i.e. the vortex edge and the subtropical barrier, manifest in **tracer** space as regions with lower PDF values separating the correlation branches (a detailed discussions follows in the next subsection). After the major SSW (see Fig. 9(c1)), the polar correlation totally disappears in **tracer** space and the tropical correlation becomes slightly weaker. **Conversely**, the PDF of the mid-latitude
410 correlation strengthens **in the time period after the major SSW**.

5.2 Tracer and physical space

Before transport and chemistry triggered by the major SSW in January 2009 will be described more quantitatively, Fig. 8 shows schematically how these physical processes can be interpreted and separated by using N₂O-O₃ correlations. Left column in Fig. 8 show the APs in physical space using

415 eq. latitudes as the meridional axis. On their right side, the corresponding tracer space is shown in
the same way as discussed in Fig. 1.

Through isentropic mixing, the APs in the mid-latitudes change their composition as they mix
with other APs isentropically transported from higher or lower latitudes (like fragments B, E, F in
Fig. 8(a1)(b1)). Consequently, mixing lines connecting the isolated correlations may appear or, when
420 intensive and persistent mixing happens, the whole correlation line inclines to one side (e.g. the thick
black correlations in Fig. 8(b2)). Moreover, the enhanced mixing also results in a decay or growth
of certain correlation branches (shown as thinned or thickened black curves in Fig. 8(b2) and (c2))
and expressing the shrinking or expanding of corresponding regions.

Conversely, if the APs are affected purely by vertical transport like strong cross-isentropic motion
425 during the SSW (i.e. by up- or downwelling), the composition of the APs (and thus their position
in tracer space) stays the same although their θ -coordinate significantly changes. As discussed in
Fig. 1 (a,b), in the absence of mixing and chemistry, an AP will not change its coordinates in the
tracer space although it will move in the physical space (e.g. vertical displacement of APs shown in
Fig. 8(b1)). Furthermore, if only APs within a limited range of potential temperature are considered,
430 the cross-isentropic transport results in an additional flux of the APs out of (export) or into (import)
the considered domain in tracer space. Such vertical export or import of APs reflects in tracer space
as vanishing or growing of certain part of correlation line (vanished parts of vortex correlation are
shown as dashed black curves in Fig. 8(b2/c2)). In the same way, export or import of APs from a
limited range of latitudes (or eq. latitudes) may influence the tracer- tracer correlation, e.g. if the
435 subtropical barrier moves toward the equator.

Generally, the major SSW itself creates vortex fragments which in the following time either can
merge and reform a new polar vortex or can be isentropically mixed with the mid-latitude air. These
two possibilities are exemplarily shown in Fig. 8(b1) and (c1) (mixing - fragments E, recovery -
fragments A, B and D). Note that in the eq. latitude space the spatially separated vortex remnants
440 form a compact and coherent circumpolar structure although smaller than the vortex at the beginning
of the winter. Finally, also chemistry can influence the N_2O-O_3 correlations as discussed in Fig. 1(c).
Particularly, halogen or NO_x -induced ozone loss would shift the polar or the surf zone correlations
downwards, whereas ozone production in the low latitudes would steepen the tropical or the surf
zone correlations.

445 Our first goal is to understand the changes in the N_2O-O_3 correlations observed by MLS before
and after the major SSW (Fig. 9(a1) to (c1)) as a result of different transport mechanisms (isentropic
mixing, meridional transport). In particular, we would like to figure out why the polar and the trop-
ical N_2O-O_3 correlations weakened after the major SSW and the mid-latitude correlation became
stronger. First, we rule out ozone chemistry by using CLaMS simulations with passively transported
450 O_3 (pO_3). At the end of this section, we will also include CLaMS results with the full stratospheric
ozone chemistry.

5.3 Isentropic mixing versus cross-isentropic transport

Two sets of CLaMS simulations, with and without mixing, are used to study the mixing-induced differences between the PDFs of the pO_3 - N_2O correlations. The results are shown in Fig. 9 (middle/bottom row for mixing/non-mixing cases). As in Fig. 9(a1)-(c1), the PDFs are calculated for the same time periods before, during and after the major SSW (from a to c). However, the range of the considered eq. latitudes is confined to 40-90°N (instead of 0-90°N shown in Fig. 9(a1) to (c1)) to separate more clearly the effect of transport from the tropics on the composition of air in the mid-latitudes (see discussion below). To provide better comparability, correlation branches of the non-mixing experiment are also depicted in the mixing case as dashed lines (and vice versa).

5.3.1 Transport from the tropics

Using such a limited range of eq. latitudes we exclude the APs on the tropical side of the subtropical barrier (that is around 20°N eq. latitude) and, it is obvious that the PDFs of the CLaMS run with mixing do not show any tropical correlation in the eq. latitude 40°- 90°N (Fig. 9 (a2) to (c2)). However, a tropical correlation was found in the non-mixing run during and after the major SSW (Fig. 9(b3/c3)) because in this idealized simulation tropical air was transported into the mid-latitudes but it has not been mixed. For a better comparison, this “artificial” tropical correlation (i.e. from Fig. 9 (b3/c3)) is also shown in Fig. 9 (b2/c2) (solid dashed line).

Thus, a clear difference in the result of the mixing and non-mixing case indicates that the tropical APs are transported from lower latitudes to mid-latitudes where they mix with the mid-latitude APs. Consequently, the slope of the surf-zone correlation moves towards the tropical correlation branch, especially between 550 K to 650 K (cf. Fig. 9 from (a2) to (c2) and (c2) with (c3)). This isentropic mixing in mid-latitudes is also consistent with the increased mixing intensity marked as A2 in Fig. 6 and Fig. 7. In contrast, an idealized, pure trajectory calculation (i.e. CLaMS without mixing) completely neglects this effect and produces N_2O - O_3 correlations which cannot be reconciled with MLS observations (i.e. for eq. latitudes 40-90°N, not shown).

5.3.2 Vortex breakup and decay

All APs which are transported along the trajectories without mixing do not change their composition and thus keep the same position in the N_2O - O_3 space unless they leave the considered range of eq. latitudes or potential temperatures. Besides the almost isentropic import of tropical APs that was mentioned in the last subsection, strong downwelling within the polar vortex, mainly during the major SSW itself, can also be diagnosed in the tracer space.

The isentropes move upwards in tracer space during the major SSW (Fig. 9 from column (a) to (b)), as a consequence of diabatic cooling (downwelling) associated with warming in the mid- and high-latitudes (see also Fig. 8). As a result of this cross-isentropic transport, the APs trans-

ported without mixing may be exported (or imported) from (or into) the considered θ -range between 450 and 700 K. E.g. such missing polar APs are obvious within the black solid squares in Fig. 9(a3/c3) defined by the N_2O values between 80-130 ppbv and O_3 between 2.7-3.5 ppmv. Note that for CLaMS with mixing these regions are filled with APs indicating that mixing in the model re-establishes parts of the correlation.

To shed more light on the ongoing processes, we plot in Fig. 10 the eq. latitudes and the potential temperature coordinates of these missing APs at the end of each of the considered time periods (from the CLaMS run without mixing). Furthermore, the APs are colored by different ranges of pO_3 and the PDFs of their eq. latitudes and θ coordinates describe their mean horizontal and vertical position during the course of the winter.

Fig. 10 shows that after the major SSW onset, most of the APs which were originally located above 450K, have been transported downwards below 450K. Therefore, the downward cross-isentropic transport within the vortex (diabatic descent) with subsequent export of the APs out of the considered potential temperature range 450-700 K is the main reason for the missing correlation inside the square of Fig. 9(c3). Moreover, most of the APs were confined inside the polar vortex before the major SSW, while after the major SSW these APs were spread almost uniformly between 40 and 90°N eq. latitude (Fig. 10c) due to chaotic advection after a complete breakup of the two vortices over eastern North America and the Atlantic (see N_2O distribution at 475 K in Fig. 4).

In the CLaMS run with mixing, the situation is stable as long as the edge of the stable vortex constitutes an effective mixing barrier (Fig. 9, column (a)). Later, during the major SSW, descent and chaotic advection have the same effect as in the idealized CLaMS simulation without mixing, i.e. part of the APs carrying the signature of the polar correlation are again eventually exported from the considered θ -range as they descend below 450 K.

However, increased mixing between these descending polar APs with the APs outside the vortex, have two additional effects: i) the signature of the polar correlation is spread to mid-latitude APs that do not descent outside the considered θ -range, such that the signature remains visible (like vortex fragment D in Fig. 8 (b1/c1)), and ii) the mixing with mid-latitude (and even tropical) APs causes the polar correlation branch to become less compact and shift toward the mid-latitude correlation branch (along the plotted isentropes (like air masses C and E in Fig. 8 (b1/c1))). These effects can be well discerned by comparing the vortex branch of the correlation for the mixed case (Fig. 9(b2/c2)) with the non-mixed case (Fig. 9(b3/c3) also denoted as dashed black curves in Fig. 9(b2/c2)).

After the breakup of the two vortices over eastern North America and Atlantic in mid-February, spreading of the polar APs across the hemisphere along with intense mixing with mostly mid-latitude and some tropical APs leads to an almost complete loss of the polar correlation branch (Fig. 9(c2)), which remains preserved only in a few unmixed vortex remnants (like fragments A, B and D in Fig. 8 (c1)). As explained by Plumb (2007), the fast and nearly hemisphere-wide isentropic mixing (as promoted by the major SSW) leads to a single compact extratropical correlation.

Note that the weak polar correlation which is present in CLaMS (see Fig. 9(c2)) is not resolved in the MLS observations. A potential explanation is the limited spatial resolution of the MLS instrument with vertical resolution of 4-6 km for N₂O and 2.5-3 km for O₃, respectively, and horizontal resolution of 200 km for both species. This means that physical structures below these spatial scales are smoothed out by the MLS instrument (an effect sometimes called optical mixing, see Appendix).

5.4 Impact of chemistry

In general, Arctic O₃ loss triggered by activated chlorine mainly occurs in late winter and spring within a sufficiently cold polar vortex. The NO_x-induced O₃ chemistry roughly follows the halogen chemistry after the vortex breakup with highest values occurring in the middle and lower stratosphere (see e.g. Solomon, 1999; WMO, 2014). To quantify the chemical effect on the N₂O-O₃ correlation, Fig. 11 shows the pO₃-N₂O correlation within 0-90°N and 450-700 K range overlaid with the correlations from the full chemistry run (dashed curves).

In the early winter, we found a small but significant amount of ozone loss in the lower stratosphere (cf. dashed curve and PDFs between 450 K and 550 K in Fig. 11 b), which is consistent with the results of Manney et al. (2015). After the onset of the warming event, only few PSCs were formed and, consequently, the subsequent, chlorine-induced ozone-loss within the polar vortex was very limited (Kuttippurath and Nikulin, 2012). This can also be inferred from the CLaMS-based correlation with pO₃ (PDFs in Fig. 11c) that is very close to the correlation based on full-chemistry O₃ (dashed curve in Fig. 11c). Besides the chlorine-catalyzed ozone loss, the remaining O₃ chemistry is of importance in our interpretation of the N₂O-O₃ correlations, especially when the temperature rises after the major SSW and thus the chemical reactions are accelerated.

Two regions (marked in Fig. 11 as A and B) of this correlation plot have been investigated in more detail regarding the chemical change of ozone. Region (A) has N₂O mixing ratios near 140 ppbv and passive ozone near 7400 ppbv on January 23rd, corresponding to a most probable location of 35°N and 650K. It is evident that here the chemistry causes ozone depletion. From the locations of 120 air parcels in this area, back-trajectories were calculated for one month along which the chemistry was calculated using the CLaMS chemistry module and additional output to analyze and quantify the contribution of the individual ozone depletion cycles (as defined by Crutzen et al., 1995) to the ozone loss term. The average ozone production over this month through oxygen photolysis was 850 ppbv which was outweighed by ozone loss of 1450 ppbv, of which about half could be attributed to NO_x-catalyzed ozone loss cycles and the remaining half equally distributed to HO_x, ClO_x and O_x cycles.

In contrast, region (B) with N₂O mixing ratios of 260 ppbv and passive ozone mixing ratios of 3800 ppbv corresponds to a most probable location of 11°N and 575 K. Here, the chemistry causes an ozone increase. A similar chemistry simulation along 132 one-month back-trajectories showed an ozone production through oxygen photolysis of 800 ppbv and net ozone depletion by 260 ppbv.

Therefore ozone production dominates **in this part of the tropics**. Since gas-phase chemical reactions
560 are temperature-dependent, we investigated **whether** the temperature anomaly (see Fig. 1b) **had** a
significant effect on ozone. An identical run along the 132 trajectories, however with temperatures set
3K higher, increased the ozone loss by 30 ppbv. The ozone production is not temperature-dependent.
A change in the ozone loss rate of 1 ppbv per day is negligible compared to the changes caused by
565 dynamics that are discussed here. Complementary to our discussion above, we find that in polar
latitudes the differences between correlations with or without chemistry are negligible indicating
minor importance of the chlorine-induced ozone-loss during the 2008/09 winter.

6 Conclusions

A remarkable major SSW in January 2009 led to strongly disturbed stratospheric dynamics which
manifested in both accelerated polar descent and tropical upwelling. During the following two weeks
570 up to the end of January, this transient signal of cross-isentropic transport propagated down from
around 1 hPa to 100 hPa. The radiative relaxation of this anomaly in diabatic heating was relatively
fast (~ 10 days) in the upper stratosphere, but took more than a month in the lower stratosphere,
which resulted in accelerated polar descent and accelerated tropical upwelling through late March
(Fig. 2).

575 Associated with the disturbed dynamical background during the major SSW, strong variability of
 N_2O and O_3 was observed by the MLS instrument. We used CLaMS to simulate transport, mixing
and chemistry to interpret the observed change of stratospheric composition. By comparison with
MLS observations of N_2O - O_3 correlations, we showed how the polar vortex edge weakened and
how the subtropical mixing barrier was affected by poleward transport followed by mixing in mid-
580 latitudes during and after the major SSW.

As an important but uncertain piece of atmospheric modeling, the mixing process could be explic-
itly and reasonably described in CLaMS simulations. The distribution of simulated mixing intensity
showed that mixing across the vortex edge and also across the subtropical barrier (above 700 K) was
enhanced after the onset of **the major SSW, triggered** by wave forcing quantified in terms of the EP
585 flux divergence.

The O_3 - N_2O correlations **have been shown** to be a useful diagnostic to separate dynamical and
chemical effects. Model results show that isentropic mixing is a key process to understand the drastic
change of stratospheric composition triggered by the major SSW: the decay of the polar O_3 - N_2O
correlation and the strengthening of the mid-latitude correlation. One month after the major SSW,
590 almost half of the vortex dissolved due to isentropic mixing, whereas the other part constituted the
germ for the formulation of a new and relatively weak vortex. Halogen-induced ozone loss within the
polar vortex was negligible in the late winter of 2008/09 winter and the dominant ozone chemistry

during and after the major SSW was the extra-tropical ozone loss due to NO_x catalytic cycles and ozone production in the tropics.

595 However, there is also a limitation of the applicability of the MLS satellite data with a vertical resolution of **a few kilometers**. As shown in the appendix, due to this limited spatial resolution, physical structures below these spatial scales and resolved by the model are smoothed out by the satellite’s averaging kernel (an effect sometimes called optical mixing). Thus, although MLS satellite data offer a very good coverage, their poor vertical resolution does not **allow us** to narrow the possible
600 range of the mixing parameters in CLaMS (i.e. of the critical Lyapunov exponent).

Finally, we can speculate that for a winter with **significant, chlorine-induced ozone loss, followed by a strong major SSW the mid-latitude air can be influenced by processed, ozone-depleted air**. Conversely, O_3 -rich air can be effectively transported into the high latitudes.

Appendix A

605 As discussed in subsection 3.2, the MLS averaging kernels were applied for both the N_2O and O_3 CLaMS output before comparing these distributions with the satellite-based observations. Given a “true” atmospheric profile x_i on n pressure levels $i = 1, \dots, n$, the averaging kernel can be understood as a smoothing procedure that determines mixing ratios at each level i by a weighted integration over all other levels with a strongest contribution of levels directly above or below the considered
610 level i . The averaging kernel is a matrix A_{ij} with most significant terms around the diagonal and with all rows i fulfilling the normalization condition $\sum_{j=1, \dots, n} A_{ij} = 1$. Thus, applying averaging kernels to model data with a high spatial resolution like CLaMS means smoothing or removing small-scale structure from the model.

In Fig. 12, the PDFs of the N_2O - O_3 correlations **are shown** for February, 15th, 2009 as observed
615 by the MLS instrument (top) and as derived from CLaMS simulations with and without smoothing by the averaging kernel (bottom). In contrast to MLS, original CLaMS output shows the polar **correlation, which disappears** if the averaging kernel is applied to CLaMS output. This polar correlation can be attributed to some remnants of the polar vortex which are resolved by CLaMS. Within the model, the lifetime of the polar correlation is about three weeks longer compared to the last time this
620 correlation was detected by the MLS instrument.

Thus, two questions arise: are these small-scale structures resolved with CLaMS realistic and **is it the N_2O or rather the O_3 -related coarse sampling of the MLS instrument that smoothes out the polar correlation of N_2O - O_3 ?** To **get an impression of how the averaging kernel smoothes out the modeled small scale filaments and tracer gradients**, Fig. 13 shows the spatial distribution of
625 N_2O vortex remnants on February, 20th, 2009 before and after applying the MLS averaging kernel procedure (**left and right column, respectively**). Here, N_2O distributions at two isentropic levels, 550

K (top row) and 650 K (bottom row) are shown, with black line denoting the strongly disturbed vortex edge.

630 N_2O and O_3 profiles from the Atmospheric Chemistry Experiment (ACE) are also used. An ACE profile crossed the potential surfaces $\theta = 550$ and 660 K on this day (red circles as the profile positions at noon on each isentrope). The nearest CLaMS APs are selected according to the same procedure as for the MLS data (see subsection 3.2). Thus, the horizontal spatial distances of ACE profiles and corresponding CLaMS profiles are less than 50 km (1.5°). The vertical resolution of ACE profiles is about 3-4 km (Bernath et al., 2005; Boone et al., 2005).

635 It can be seen that the vertical variability of the untreated CLaMS simulation of N_2O is confirmed by the corresponding ACE profile (top panel in Fig. 14). On the other hand, this variability is removed from the CLaMS simulation if the MLS averaging kernel is applied and, consequently, the comparison with the ACE observations becomes worse. However, the smoothing does not significantly change the O_3 profiles (bottom panel in Fig. 14). This is mainly because the vertical variability of O_3 is much smaller if compared with the N_2O profile and not because of a higher vertical resolution of the MLS-based O_3 observations (i.e. 2.5-3 km for O_3 versus 5-6 km for N_2O).

645 This can also be inferred from the comparison of the horizontal and vertical gradients of both tracers. Within the vertical range between $\theta = 400$ and 800 K, the horizontal variability of N_2O across the vortex edge (~ 100 ppbv) is comparable with the vertical variability (~ 150 ppbv), whereas O_3 gradient across polar vortex edge (around $1\sim 2$ ppmv) is much smaller than its vertical gradient in stratosphere (~ 5 ppmv). Therefore, the filaments or vortex remnants which are not completely mixed, and which are mainly formed by the horizontal transport, contribute to a more pronounced vertical variability of N_2O than of the O_3 profiles.

Acknowledgements. We thank ECMWF for providing reanalysis data and MLS team for providing the N_2O and O_3 data. Excellent programming support was provided by N. Thomas. We thank the Atmospheric Chemistry Experiment (ACE) team, a Canadian-led mission mainly supported by the Canadian Space Agency and the Natural Sciences and Engineering Research Council of Canada, for providing the N_2O and O_3 data. We thank Eric Ray, Gloria Manney and an anonymous reviewer for their very thoughtful and helpful reviews.

References

- 655 Andrews, D. G., Holton, J. R., and Leovy, C. B.: *Middle Atmosphere Dynamics*, Academic Press, San Diego, USA, 1987.
- Ayarzagüena, B., Langematz, U., and Serrano, E.: Tropospheric forcing of the stratosphere: A comparative study of the two different major stratospheric warmings in 2009 and 2010, *Journal of Geophysical Research: Atmospheres* (1984–2012), 116, 2011.
- 660 Bernath, P., McElroy, C., Abrams, M., Boone, C., Butler, M., Camy-Peyret, C., Carleer, M., Clerbaux, C., Coheur, P., Colin, R., DeCola, P., Bernath, P., McElroy, C., Abrams, M., Boone, C., Butler, M., Camy-Peyret, C., Carleer, M., Clerbaux, C., Coheur, P., Colin, R., DeCola, P., DeMaziere, M., Drummond, J., Dufour, D., Evans, W., Fast, H., Fussen, D., Gilbert, K., Jennings, D., Llewellyn, E., Lowe, R., Mahieu, E., McConnell, J., McHugh, M., McLeod, S., Michaud, R., Midwinter, C., Nassar, R., Nichitiu, F., Nowlan, C., Rinsland, C.,
- 665 Rochon, Y., Rowlands, N., Semeniuk, K., Simon, P., Skelton, R., Sloan, J., Soucy, M., Strong, K., Tremblay, P., Turnbull, D., Walker, K., Walkty, I., Wardle, D., Wehrle, V., Zander, R., and Zou, J.: Atmospheric Chemistry Experiment (ACE): Mission overview, *Geophys. Res. Lett.*, 32, doi:10.1029/2005GL022386, 2005.
- Boone, C. D., Nassar, R., Walker, K. A., Rochon, Y., McLeod, S. D., Rinsland, C. P., and Bernath, P. F.: Retrievals for the atmospheric chemistry experiment Fourier-transform spectrometer, *Applied optics*, 44,
- 670 7218–7231, 2005.
- Butler, A. H., Seidel, D. J., Hardiman, S. C., Butchart, N., Birner, T., and Match, A.: Defining sudden stratospheric warmings, *Bulletin of the American Meteorological Society*, doi:0.1175/BAMS-D-13-00173.1, 2015.
- Charlton, A. J. and Polvani, L. M.: A new look at stratospheric sudden warmings. Part I: Climatology and
- 675 modeling benchmarks, *Journal of Climate*, 20, 449–469, 2007.
- Christiansen, B.: Downward propagation of zonal mean zonal wind anomalies from the stratosphere to the troposphere: Model and reanalysis, *Journal of Geophysical Research: Atmospheres* (1984–2012), 106, 27 307–27 322, 2001.
- Crutzen, P. J., Groö, J.-U., Brühl, C., Müller, R., and Russell III, J. M.: A Reevaluation of the ozone budget
- 680 with HALOE UARS data: No evidence for the ozone deficit, *Science*, 268, 705–708, 1995.
- Dee, D. P., Uppala, S. M., Simmons, A. J., Berrisford, P., Poli, P., Kobayashi, S., Andrae, U., Balmaseda, M. A., Balsamo, G., Bauer, P., Bechtold, P., Beljaars, A. C. M., van de Berg, L., Bidlot, J., Bormann, N., Delsol, C., Dragani, R., Fuentes, M., Geer, A. J., Haimberger, L., Healy, S. B., Hersbach, H., Holm, E. V., Isaksen, I., Kallberg, P., Kohler, M., Matricardi, M., McNally, A. P., Monge-Sanz, B. M., Morcrette, J. J.,
- 685 Park, B. K., Peubey, C., de Rosnay, P., Tavolato, C., Thepaut, J. N., and Vitart, F.: The ERA-Interim reanalysis: configuration and performance of the data assimilation system, *Q. J. R. Meteorol. Soc.*, 137, 553–597, doi:10.1002/qj.828, 2011.
- Dickinson, R. E.: On the exact and approximate linear theory of vertically propagating planetary Rossby waves forced at a spherical lower boundary, *Monthly Weather Review*, 96, 405–415, 1968.
- 690 Edouard, S., Legras, B., Lefèvre, F., and Eymard, R.: The effect of small-scale inhomogeneities on ozone depletion in the Arctic, *Nature*, 384, 444–447, 1996.
- Eliassen, A.: Slow thermally or frictionally controlled meridional circulation in a circular vortex, *Astrophysica Norvegica*, 5, 19, 1951.

- 695 Fairlie, T. D., Pierce, R. B., Grose, W. L., Lingenfelter, G., Loewenstein, M., and Podolske, J. R.: Lagrangian forecasting during ASHOE/MAESA: Analysis of predictive skill for analyzed and reverse-domain-filled potential vorticity, *J. Geophys. Res.*, 102, 13 169–13 182, 1997.
- Gómez-Escolar, M., Calvo, N., Barriopedro, D., and Fueglistaler, S.: Tropical Response to Stratospheric Sudden Warmings and its modulation by the QBO, *Journal of Geophysical Research: Atmospheres*, doi:10.1002/2013JD020560, 2014.
- 700 Groöß, J.-U., Günther, G., Müller, R., Konopka, P., Bausch, S., Schlager, H., Voigt, C., Volk, C. M., and Toon, G. C.: Simulation of denitrification and ozone loss for the Arctic winter 2002/2003, *Atmos. Chem. Phys.*, 5, 1437–1448, 2005.
- Groöß, J.-U., Konopka, P., and Müller, R.: Ozone chemistry during the 2002 Antarctic vortex split, *J. Atmos. Sci.*, 62, 860–870, 2005.
- 705 Groöß, J.-U., Engel, I., Borrmann, S., Frey, W., Günther, G., Hoyle, C., Kivi, R., Luo, B., Molleker, S., Peter, T., Pitts, M. C., Schlager, H., Stiller, G., Vömel, H., Walker, K. A., and Müller, R.: Nitric acid trihydrate nucleation and denitrification in the Arctic stratosphere, *acp*, 14, 1055–1073, 2014.
- Harada, Y., Goto, A., Hasegawa, H., Fujikawa, N., Naoe, H., and Hirooka, T.: A major stratospheric sudden warming event in January 2009, *Journal of the Atmospheric Sciences*, 67, 2052–2069, 2010.
- 710 Haynes, P. and Shuckburgh, E.: Effective diffusivity as a diagnostic of atmospheric transport, 1, *Stratosphere, J. Geophys. Res.*, 105, 22 777–22 794, 2000.
- Hegglin, M. I. and Shepherd, T. G.: O₃-N₂O correlations from the Atmospheric Chemistry Experiment: Revisiting a diagnostic of transport and chemistry in the stratosphere, *J. Geophys. Res.*, D19301, doi:10.1029/2006JD008281, 2007.
- 715 Hitchcock, P. and Shepherd, T. G.: Zonal-mean dynamics of extended recoveries from stratospheric sudden warmings, *Journal of the Atmospheric Sciences*, 70, 688–707, 2013.
- Holton, J. R., Haynes, P., McIntyre, M. E., Douglass, A. R., Rood, R. B., and Pfister, L.: Stratosphere-troposphere exchange, *Rev. Geophys.*, 33, 403–439, 1995.
- Hoppe, C. M., Hoffmann, L., Konopka, P., Groöß, J.-U., Ploeger, F., Günther, G., Jöckel, P., and Müller, R.: The
720 implementation of the CLaMS Lagrangian transport core into the chemistry climate model EMAC 2.40.1: application on age of air and transport of long-lived trace species, *Geoscientific Model Development*, 7, 2639–2651, 2014.
- Khosrawi, F., Groöß, J.-U., Müller, R., Konopka, P., Kouker, W., Ruhnke, R., Reddman, T., and Riese, M.:
725 Intercomparison between Lagrangian and Eulerian simulations of the development of mid-latitude streamers as observed by CRISTA, *Atmospheric Chemistry and Physics*, 5, 85–95, 2005.
- Konopka, P., Groöß, J.-U., Bausch, S., Müller, R., McKenna, D. S., Morgenstern, O., and Orsolini, Y.: Dynamics and chemistry of vortex remnants in late Arctic spring 1997 and 2000: Simulations with the Chemical Lagrangian Model of the Stratosphere (CLaMS), *Atmos. Chem. Phys.*, 3, 839–849, 2003.
- Konopka, P., Steinhorst, H.-M., Groöß, J.-U., Günther, G., Müller, R., Elkins, J. W., Jost, H.-J., Richard, E.,
730 Schmidt, U., Toon, G., and McKenna, D. S.: Mixing and Ozone Loss in the 1999-2000 Arctic Vortex: Simulations with the 3-dimensional Chemical Lagrangian Model of the Stratosphere (CLaMS), *J. Geophys. Res.*, 109, D02315, doi:10.1029/2003JD003792, 2004.

- Konopka, P., Grooß, J.-U., Hoppel, K. W., Steinhorst, H.-M., and Müller, R.: Mixing and chemical ozone loss during and after the Antarctic polar vortex major warming in September 2002, *J. Atmos. Sci.*, 62, 848–859, 2005.
- 735 Konopka, P., Günther, G., Müller, R., dos Santos, F. H. S., Schiller, C., Ravegnani, F., Ulanovsky, A., Schlager, H., Volk, C. M., Viciani, S., Pan, L. L., McKenna, D.-S., and Riese, M.: Contribution of mixing to upward transport across the tropical tropopause layer (TTL), *Atmos. Chem. Phys.*, 7, 3285–3308, 2007.
- Konopka, P., Grooß, J.-U., Günther, G., Ploeger, F., Pommrich, R., Müller, R., and Livesey, N.: Annual cycle of ozone at and above the tropical tropopause: observations versus simulations with the Chemical Lagrangian Model of the Stratosphere (CLaMS), *Atmos. Chem. Phys.*, 10, 121–132, doi:10.5194/acp-10-121-2010, <http://www.atmos-chem-phys.net/10/121/2010/>, 2010.
- 740 Kuttippurath, J. and Nikulin, G.: A comparative study of the major sudden stratospheric warmings in the Arctic winters 2003/2004–2009/2010, *Atmospheric Chemistry and Physics*, 12, 8115–8129, 2012.
- 745 Labitzke, K. and Kunze, M.: On the remarkable Arctic winter in 2008/2009, *Journal of Geophysical Research: Atmospheres* (1984–2012), 114, D00I02, doi:10.1029/2009JD012273, 2009.
- Lahoz, W., Errera, Q., Viscardy, S., and Manney, G.: The 2009 stratospheric major warming described from synergistic use of BASCOE water vapour analyses and MLS observations, *Atmospheric Chemistry and Physics*, 11, 4689–4703, 2011.
- 750 Lemmen, C., Müller, R., Konopka, P., and Dameris, M.: Critique of the tracer-tracer correlation technique and its potential to analyse polar ozone loss in chemistry-climate models, *J. Geophys. Res.*, 111, D18307, doi:10.1029/2006JD007298, 2006.
- Livesey, N., Logan, J., Santee, M., Waters, J., Doherty, R., Read, W., Froidevaux, L., and Jiang, J.: Interrelated variations of O₃, CO and deep convection in the tropical/subtropical upper troposphere observed by the Aura Microwave Limb Sounder (MLS) during 2004–2011, *Atmospheric Chemistry and Physics*, 13, 579–598, 2013.
- 755 Livesey, N. J., Read, W. G., Froidevaux, L., Lambert, A., Manney, G. L., Pumphrey, H. C., Santee, M. L., Schwartz, M. J., Wang, S., Cofield, R. E., Cuddy, D. T., Fuller, R. A., Jarnot, R. F., Jiang, J. H., Knosp, B. W., Stek, P. C., Wagner, P. A., and Wu, D. L.: Version 3.3 Level 2 data quality and description document, JPL D-33509, 2011.
- 760 Mahowald, N. M., Plumb, R. A., Rasch, P. J., del Corral, J., and Sassi, F.: Stratospheric transport in a three-dimensional isentropic coordinate model, *J. Geophys. Res.*, 107, 4254, doi:10.1029/2001JD001313, 2002.
- Manney, G. L., Bird, J. C., Donovan, D. P., Duck, T. J., Whiteway, J. A., Pal, S. R., and Carswell, A. I.: Modeling ozone laminae in ground-based Arctic wintertime observations using trajectory calculations and satellite data, *J. Geophys. Res.*, 103, 5797–5814, 1998.
- 765 Manney, G. L., Krüger, K., Sabutis, J. L., Amina Sena, S., and Pawson, S.: The remarkable 2003–2004 winter and other recent warm winters in the Arctic stratosphere in the late 1990s, *J. Geophys. Res.*, 110, D04107, doi:10.1029/2004JD005367, 2005.
- Manney, G. L., Krüger, K., Pawson, S., Minschwaner, K., Schwartz, M. J., Daffer, W. H., Livesey, N. J., Mlynczak, M. G., Remsberg, E. E., Russell, J. M., and Water, J. W.: The evolution of the stratopause during the 2006 major warming: Satellite data and assimilated meteorological analyses, *Journal of Geophysical Research: Atmospheres* (1984–2012), 113, doi:10.1029/2007JD009097, 2008.
- 770

- Manney, G. L., Harwood, R. S., MacKenzie, I. A., Minschwaner, K., Allen, D. R., Santee, M. L., Walker, K. A.,
Hegglin, M. I., Lambert, A., Pumphrey, H. C., Bernath, P. F., Boone, C. D., Schwartz, M. J., Livesey, N. J.,
775 Daffer, W. H., and Fuller, R. A.: Satellite observations and modeling of transport in the upper troposphere
through the lower mesosphere during the 2006 major stratospheric sudden warming, *Atmos. Chem. Phys.*,
9, 4775–4795, doi:10.5194/acp-9-4775-2009, 2009a.
- Manney, G. L., Schwartz, M. J., Krüger, K., Santee, M. L., Pawson, S., Lee, J. N., Daffer, W. H., Fuller,
R. A., and Livesey, N. J.: Aura Microwave Limb Sounder observations of dynamics and transport during
780 the record-breaking 2009 Arctic stratospheric major warming, *Geophysical Research Letters*, 36, L12 815,
doi:10.1029/2009GL038586, 2009b.
- Manney, G. L., Lawrence, Z., Santee, M., Livesey, N., Lambert, A., and Pitts, M.: Polar processing in a split
vortex: Arctic ozone loss in early winter 2012/2013, *Atmospheric Chemistry and Physics*, 15, 5381–5403,
2015.
- 785 Matsuno, T.: A dynamical model of the stratospheric sudden warming, *Journal of the Atmospheric Sciences*,
28, 1479–1494, 1971.
- McIntyre, M. E. and Palmer, T. N.: Breaking planetary waves in the stratosphere, *Nature*, 305, 593–600, 1983.
- McKenna, D. S., Groß, J.-U., Günther, G., Konopka, P., Müller, R., Carver, G., and Sasano, Y.: A new Chemical
Lagrangian Model of the Stratosphere (CLaMS): 2. Formulation of chemistry scheme and initialization,
790 *J. Geophys. Res.*, 107, 4256, doi:10.1029/2000JD000113, 2002a.
- McKenna, D. S., Konopka, P., Groß, J.-U., Günther, G., Müller, R., Spang, R., Offermann, D., and Orsolini, Y.:
A new Chemical Lagrangian Model of the Stratosphere (CLaMS): 1. Formulation of advection and mixing,
J. Geophys. Res., 107, 4309, doi:10.1029/2000JD000114, 2002b.
- Michelsen, H. A., Manney, G. L., Gunson, M. R., and Zander, R.: Correlations of stratospheric abundances of
795 NO_y , O_3 , N_2O , and CH_4 derived from ATMOS measurements, *J. Geophys. Res.*, 103, 28 347–28 359, 1998.
- Mlynczak, M. G., Mertens, C. J., Garcia, R. R., and Portmann, R. W.: A detailed evaluation of the stratospheric
heat budget: 2. Global radiation balance and diabatic circulations, *J. Geophys. Res.*, 104, 6039–6066, 1999.
- Müller, R., Crutzen, P. J., Groß, J.-U., Brühl, C., Russell III, J. M., and Tuck, A. F.: Chlorine activation and
ozone depletion in the Arctic vortex: Observations by the Halogen Occultation Experiment on the Upper
800 Atmosphere Research Satellite, *J. Geophys. Res.*, 101, 12 531–12 554, 1996.
- Müller, R., Schmidt, U., Engel, A., McKenna, D. S., and Proffitt, M. H.: The O_3 – N_2O relationship from balloon-
borne observations as a measure of Arctic ozone loss in 1991/92, *Q. J. R. Meteorol. Soc.*, 127, 1389–1412,
2001.
- Müller, R., Tilmes, S., Konopka, P., Groß, J.-U., and Jost, H.-J.: Impact of mixing and chemical change on
805 ozone-tracer relations in the polar vortex, *Atmos. Chem. Phys.*, 5, 3139–3151, 2005.
- Nash, E. R., Newman, P. A., Rosenfield, J. E., and Schoeberl, M. R.: An objective determination of the polar
vortex using Ertel’s potential vorticity, *J. Geophys. Res.*, 101, 9471–9478, 1996.
- Newman, P. A., Nash, E. R., and Rosenfield, J. E.: What controls the temperature of the Arctic stratosphere
during the spring?, *J. Geophys. Res.*, 106, 19 999–20 010, doi:10.1029/2000JD000061, 2001.
- 810 Orsolini, Y. J., Hansen, G., Hoppe, U. P., Manney, G. L., and Fricke, K. H.: Dynamical modelling of wintertime
lidar observations in the Arctic, *Q. J. R. Meteorol. Soc.*, 123, 785–800, 1997.

- Orsolini, Y. J., Urban, J., Murtagh, D. P., Lossow, S., and Limpasuvan, V.: Descent from the polar mesosphere and anomalously high stratopause observed in 8 years of water vapor and temperature satellite observations by the Odin Sub-Millimeter Radiometer, *J. Geophys. Res.*, 115, 2010.
- 815 Ploeger, F., Konopka, P., Günther, G., J.-U-Groß, and Müller, R.: Impact of the vertical velocity scheme on modeling transport across the tropical tropopause layer, *J. Geophys. Res.*, 115, doi:10.1029/2009JD012023, 2010.
- Ploeger, F., Günther, G., Konopka, P., Fueglistaler, S., Müller, R., Hoppe, C., Kunz, A., Spang, R., Groß, J.-U., and Riese, M.: Horizontal water vapor transport in the lower stratosphere from subtropics to high latitudes
820 during boreal summer, *J. Geophys. Res.*, 118, 8111–8127, doi:10.1002/jgrd.50636, 2013.
- Plumb, R. A.: A “tropical pipe” model of stratospheric transport, *J. Geophys. Res.*, 101, 3957–3972, 1996.
- Plumb, R. A.: Tracer interrelationships in the stratosphere, *Rev. Geophys.*, 45, RG4005, doi:10.1029/2005RG000179, 2007.
- Plumb, R. A. and Bell, R. C.: A model of the quasi-biennial oscillation on an equatorial beta-plane, *Quarterly
825 Journal of the Royal Meteorological Society*, 108, 335–352, 1982.
- Polvani, L. M., Waugh, D., and Plumb, R. A.: On the subtropical edge of the stratospheric surf zone, *Journal of the atmospheric sciences*, 52, 1288–1309, 1995.
- Pommrich, R., Müller, R., Groß, J.-U., Konopka, P., Ploeger, F., Vogel, B., Tao, M., Hoppe, C., Günther, G., Spelten, N., et al.: Tropical troposphere to stratosphere transport of carbon monoxide and long-lived trace
830 species in the Chemical Lagrangian Model of the Stratosphere (CLaMS), *Geoscientific Model Development*, 7, 2895–2916, 2014.
- Proffitt, M. H., Margitan, J. J., Kelly, K. K., Loewenstein, M., Podolske, J. R., and Chan, K. R.: Ozone loss in the Arctic polar vortex inferred from high altitude aircraft measurements, *Nature*, 347, 31–36, 1990.
- Punge, H. J., Konopka, P., Giorgetta, M. A., and Müller, R.: Effects of the quasi-biennial oscillation on low-
835 latitude transport in the stratosphere derived from trajectory calculations, *J. Geophys. Res.*, 114, D03102, doi:10.1029/2008JD010518, 2009.
- Randel, W. J., Garcia, R. R., and Wu, F.: Time-Dependent Upwelling in the Tropical Lower Stratosphere Estimated from the Zonal-Mean Momentum Budget, *J. Atmos. Sci.*, 59, 2141–2152, 2002.
- Ray, E. A., Moore, F. L., Elkins, J. W., Hurst, D. F., Romashkin, P. A., Dutton, G. S., and Fahey, D. W.: Descent
840 and mixing in the 1999-2000 northern polar vortex inferred from in situ tracer measurements, *J. Geophys. Res.*, 107, 8285, doi:10.1029/2001JD000961, 2002.
- Riese, M., Ploeger, F., Rap, A., Vogel, B., Konopka, P., Dameris, M., and Forster, P. M.: Impact of uncertainties in atmospheric mixing on simulated UTLS composition and related radiative effects, *J. Geophys. Res.*, 117, D16, doi:doi:10.1029/2012JD017751, 2012.
- 845 Sankey, D. and Shepherd, T. G.: Correlations of long-lived chemical species in a middle atmosphere general circulation model, *J. Geophys. Res.*, 108, 4494, doi:10.1029/2002JD002799, 2003.
- Shuckburgh, E., Norton, W., Iwi, A., and Haynes, P.: Influence of the quasi-biennial oscillation on isentropic transport and mixing in the tropics and subtropics, *J. Geophys. Res.*, 106, 14 327–14 337, 2001.
- Sofieva, V., Kalakoski, N., Verronen, P., Päivärinta, S.-M., Kyrölä, E., Backman, L., and Tamminen, J.: Polar-
850 night O₃, NO₂ and NO₃ distributions during sudden stratospheric warmings in 2003–2008 as seen by GOMOS/Envisat, *Atmospheric Chemistry and Physics*, 12, 1051–1066, 2012.

- Solomon, S.: Stratospheric ozone depletion: A review of concepts and history, *Rev. Geophys.*, 37, 275–316, doi:10.1029/1999RG900008, 1999.
- Steinhorst, H.-M., Konopka, P., Günther, G., and Müller, R.: How permeable is the edge of the Arctic vortex —
855 Model studies of the winter 1999–2000, *J. Geophys. Res.*, 110, D06105, doi:10.1029/2004JD005268, 2005.
- Sutton, R. T., Maclean, H., Swinbank, R., O’Neill, A., and Taylor, F. W.: High-resolution stratospheric tracer fields estimated from satellite observations using Lagrangian trajectory calculations, *J. Atmos. Sci.*, 51, 2995–3005, 1994.
- Taguchi, M.: Latitudinal Extension of Cooling and Upwelling Signals Associated with Stratospheric Sudden
860 Warmings, *Journal of the Meteorological Society of Japan. Ser. II*, 89, 571–580, 2011.
- Tilmes, S., Müller, R., Engel, A., Rex, M., and Russell III, J.: Chemical ozone loss in the Arctic and Antarctic stratosphere between 1992 and 2005, *Geophys. Res. Lett.*, 33, L20812, doi:10.1029/2006GL026925, 2006.
- Tuck, A. F.: Depletion of Antarctic ozone, *Nature*, 321, 729–730, 1986.
- Volk, C. M., Elkins, J. W., Fahey, D. W., Salawitch, R. J., Dutton, G. S., Gilligan, J. M., Proffitt, M. H., Loewenstein, M., Podolske, J. R., Minschwaner, K., Margitan, J. J., and Chan, K. R.: Quantifying transport between
865 the tropical and mid-latitude lower stratosphere, *Science*, 272, 1763–1768, 1996.
- WMO: Scientific Assessment of Ozone Depletion: 2014, Global Ozone Research and Monitoring Project–Report No. 56, Geneva, Switzerland, 2014.

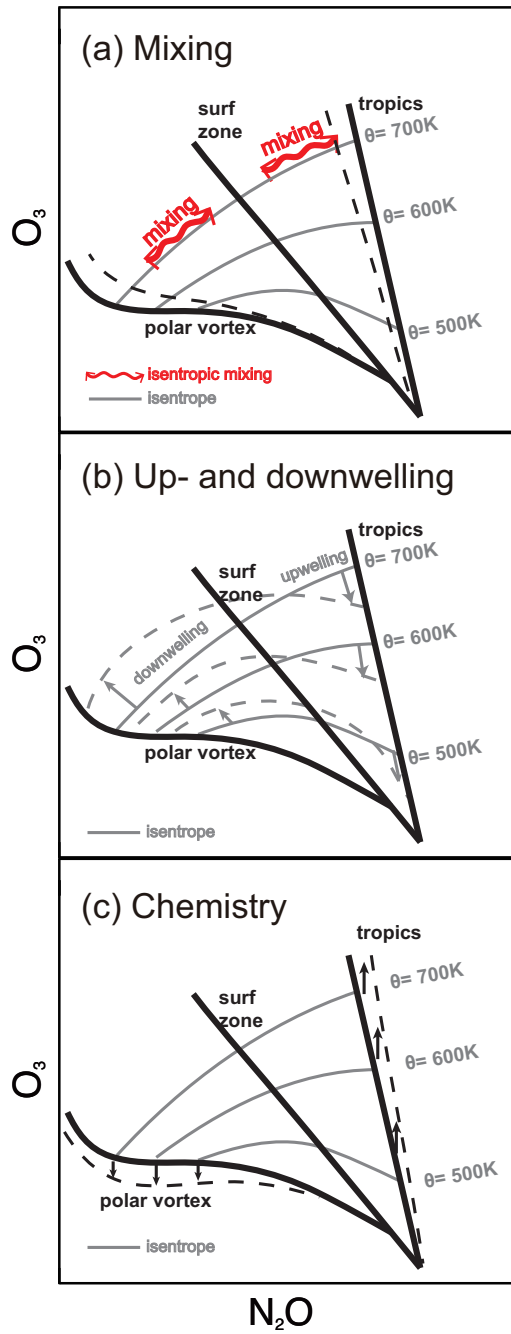


Figure 1. Schematic diagram shown the influences of (a) mixing, (b) up- and downwelling and (c) chemistry on N_2O - O_3 correlations.

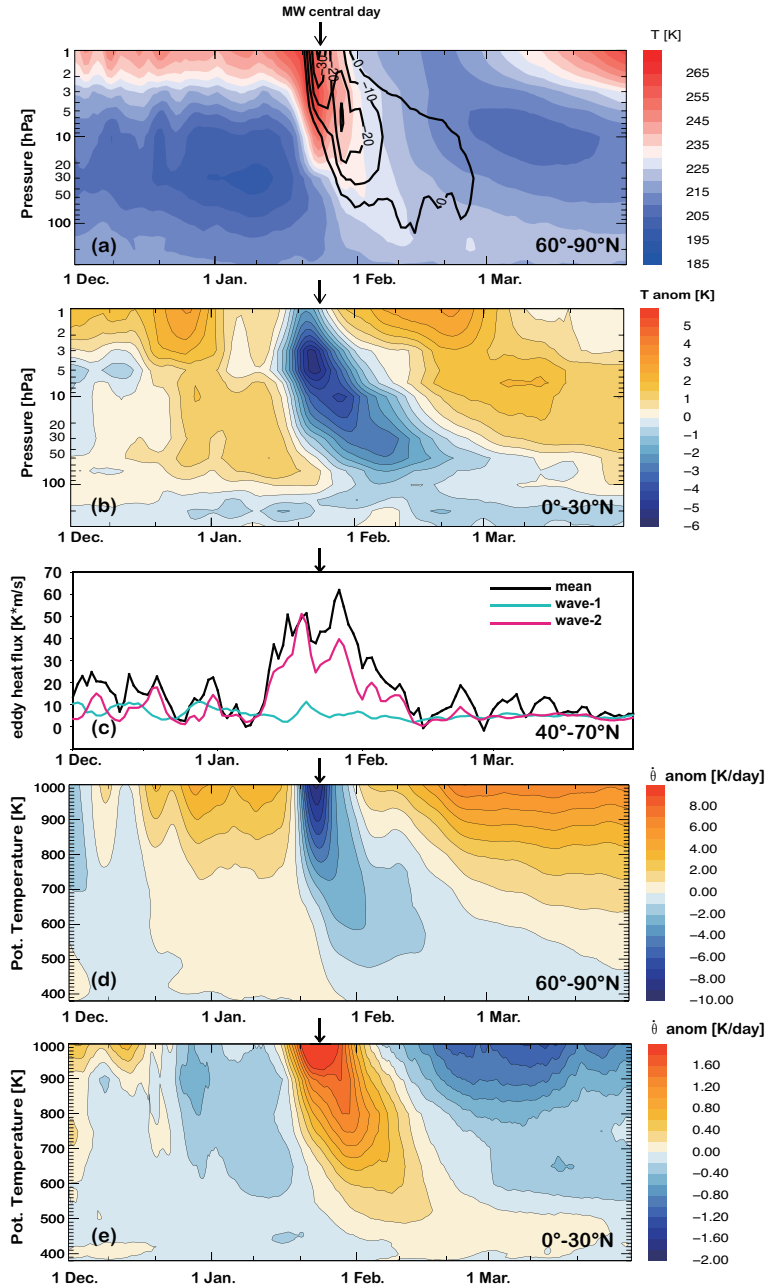


Figure 2. (a) Polar cap area weighted mean temperature ($60^\circ - 90^\circ\text{N}$) overlaid with zonal mean easterlies at 60°N (black contours in m/s), (b) tropical zonal mean temperature anomaly from the 24-year climatology ($0^\circ - 20^\circ\text{N}$), (c) eddy heat flux ($40^\circ - 70^\circ\text{N}$, black) on 100 hPa and its decomposition into wave-1 (blue) and wave-2 (red) components (d) polar mean ($60^\circ - 90^\circ\text{N}$) anomaly of the heating rates from the 24-year climatology $Q = d\theta/dt = \dot{\theta}$ (for more details see the text), (e) same as (d) but for $0^\circ - 30^\circ\text{N}$. The figures are based on the ERA-interim reanalysis.

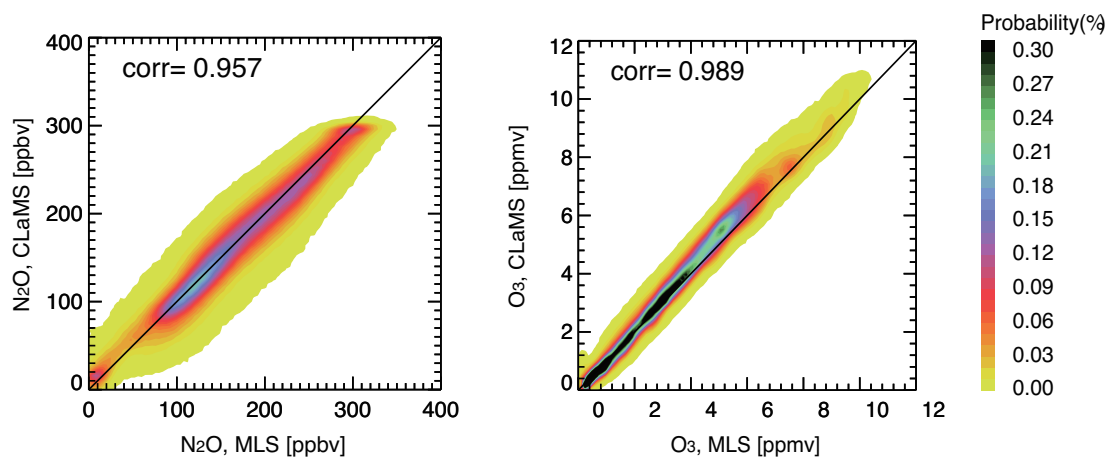


Figure 3. PDFs of MLS observations and CLaMS reference simulation for the entire simulation period from December 1st, 2008 to April 1st, 2009 for APs in the northern hemisphere with $400 \text{ K} < \theta < 1000 \text{ K}$ (left: N₂O, right: O₃).

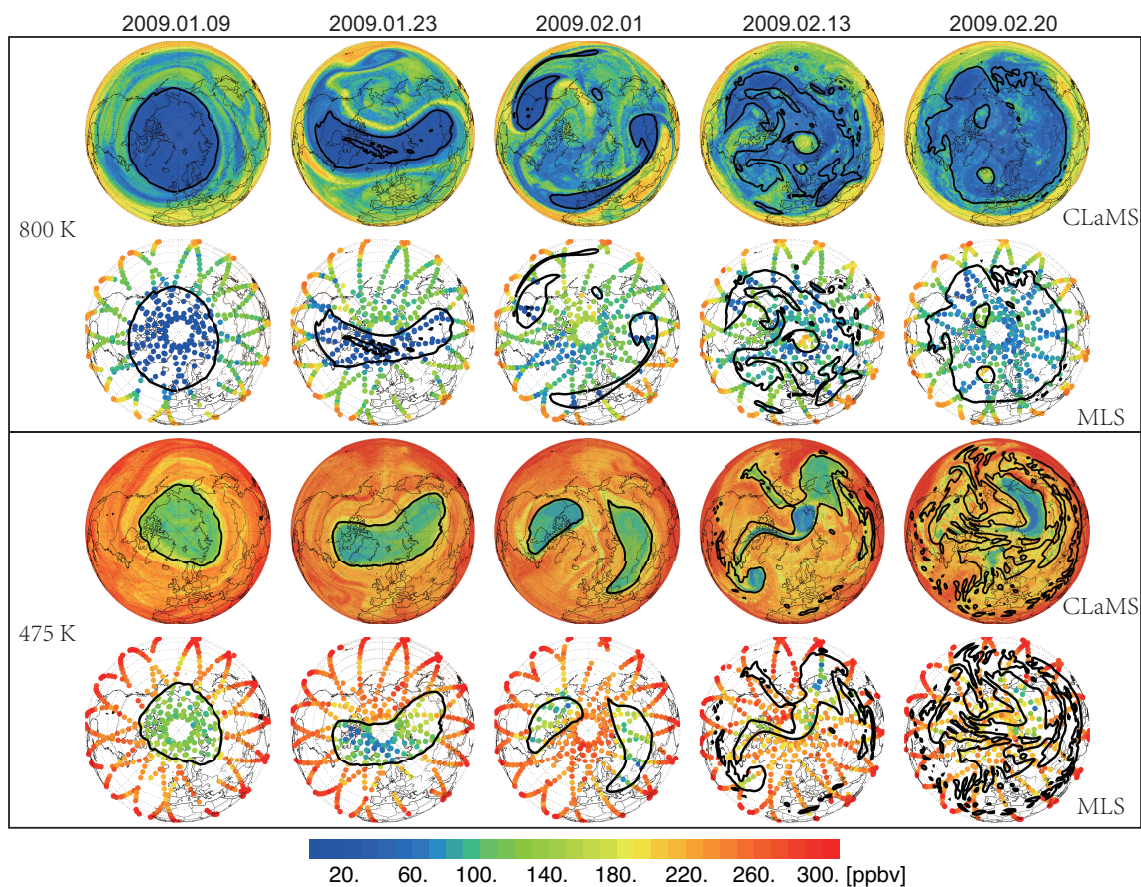


Figure 4. N_2O distribution at $\theta = 800$ K (top 2 rows) and 475 K (bottom 2 rows) interpolated from CLaMS simulation and MLS observations for five selected days in 2009 before and after the major SSW event. Nash's criteria (Nash et al., 1996) is applied to define the edge of the polar vortex shown as the black contours. According to this method, the vortex edge is identified as the maximum PV gradient with respect to equivalent latitude constrained by the location of the maximum wind jet calculated along equivalent latitudes.

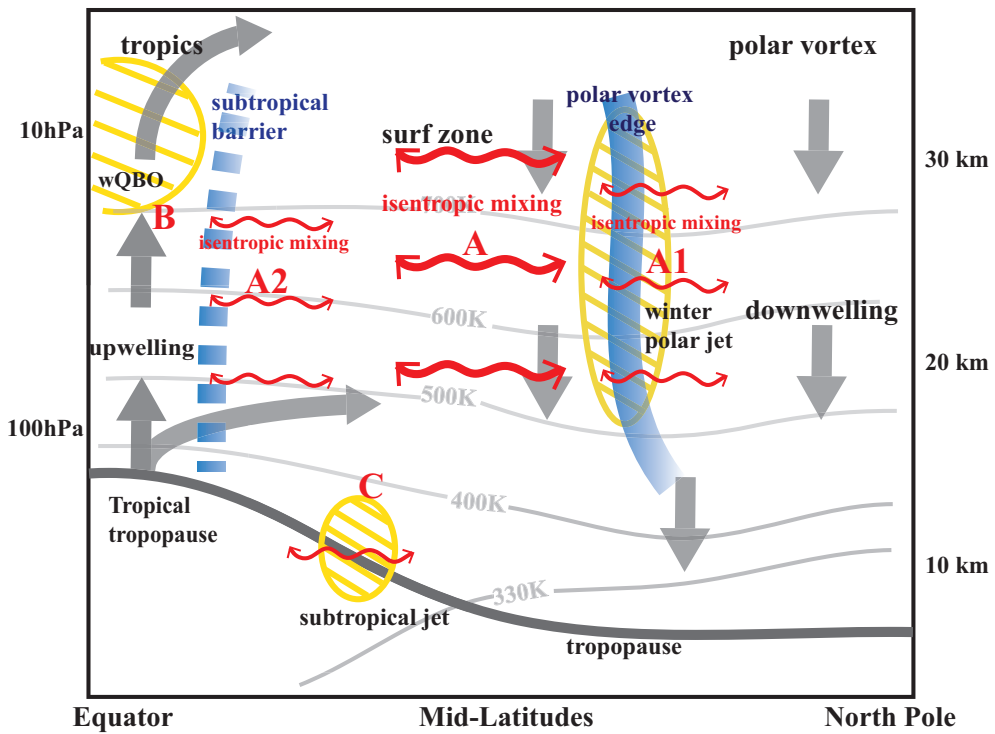


Figure 5. Schematic picture of transport and mixing processes in the winter stratosphere. The thick blue lines show the barriers, the gray arrows indicate the direction of the BD circulation. Yellow shaded areas stand for strong westerlies. Red two-headed arrows indicate isentropic mixing, with thicker and thinner arrows showing stronger mixing in the surf zone and weaker mixing across the transport barriers, respectively. For a better overview, the tropopause with the subtropical jet are also marked.

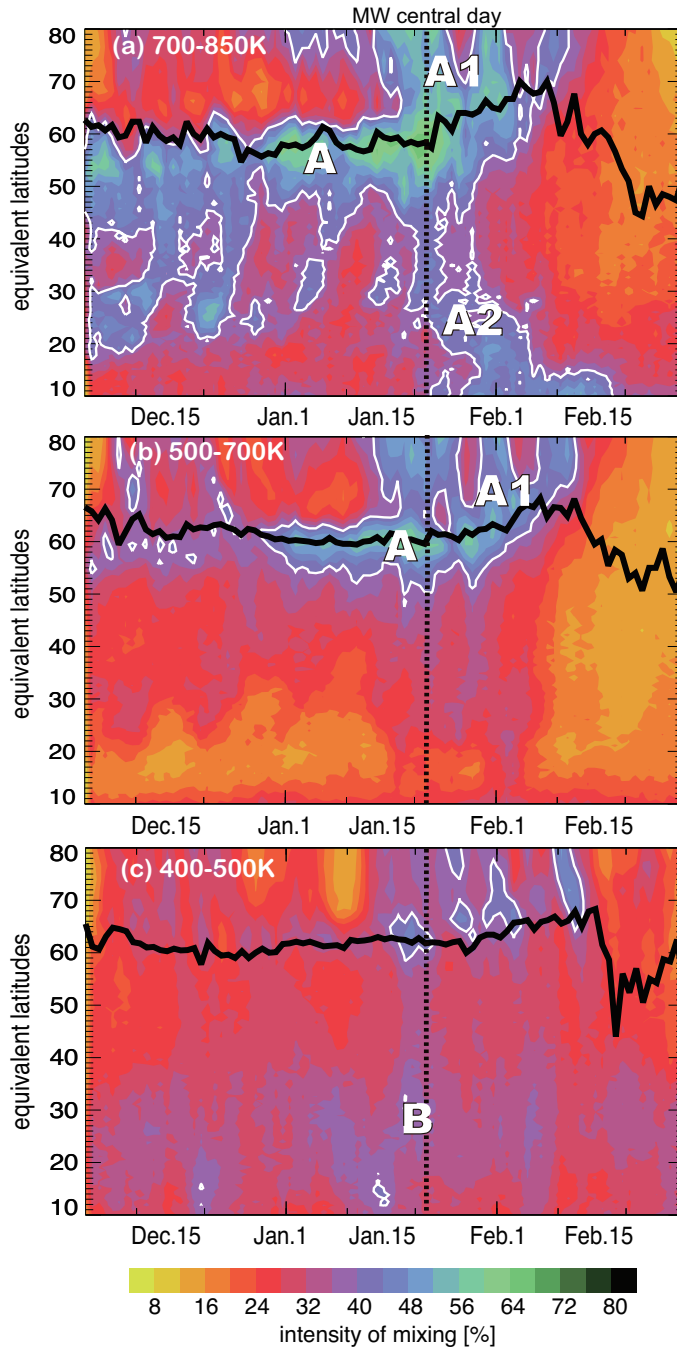


Figure 6. CLaMS zonal mean mixing intensity within 3 layers: (a) 700 - 850 K, (b) 500 - 700 K, (c) 400 - 500 K overlaid by the location of the vortex edge (thick black lines (Nash et al., 1996)) and the white contours indicate the mixing intensity of 40%. The letters mark the regions of high mixing intensity and correspond to the letters in Fig. 7.

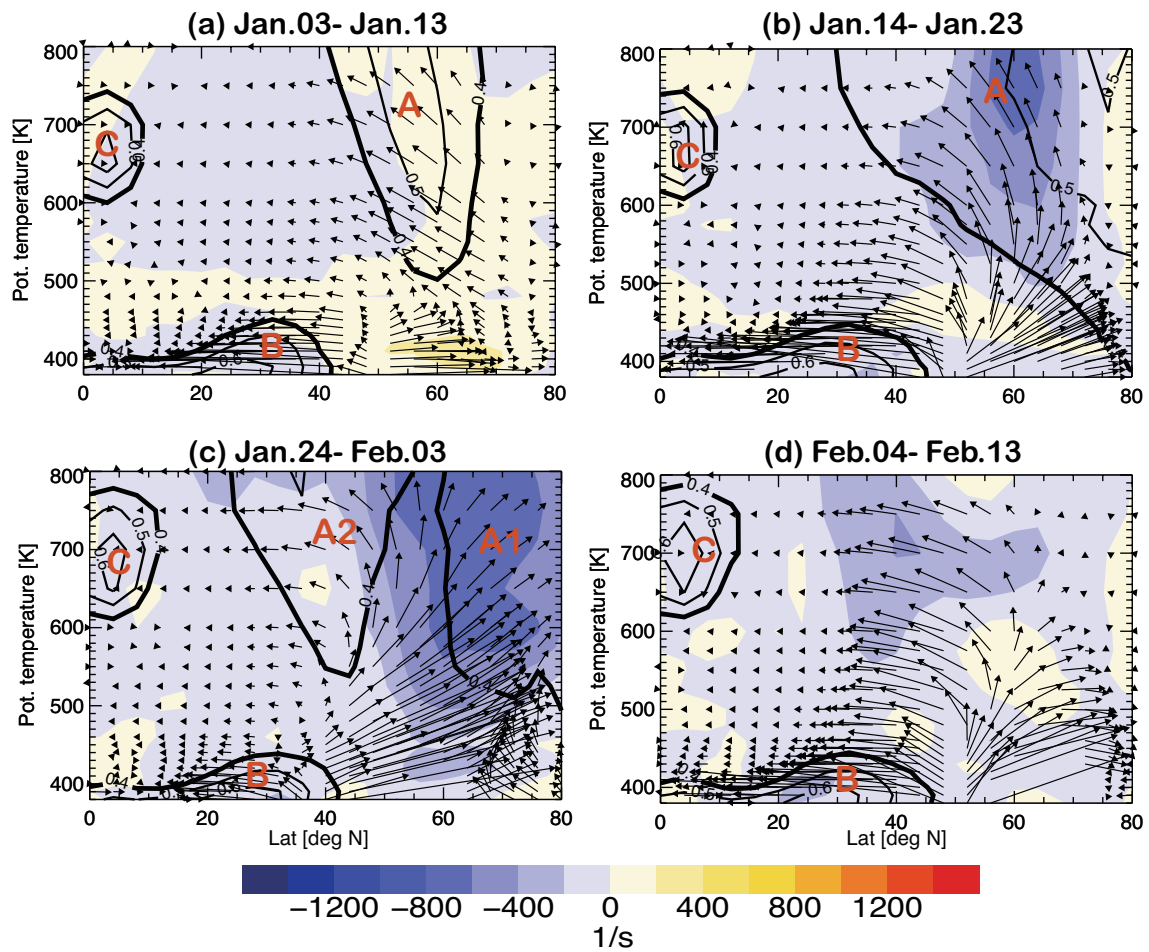


Figure 7. EP flux (arrows) and its divergence (colored bluish). Black contours indicate the mixing intensity larger than 0.4. The panels (a)-(d) show mean values averaged over 4 time periods: (a) Jan. 03 - Jan. 13 (b) Jan. 14 - Jan. 23 (c) Jan. 24 - Feb. 03 (d) Feb. 04 - Feb. 13

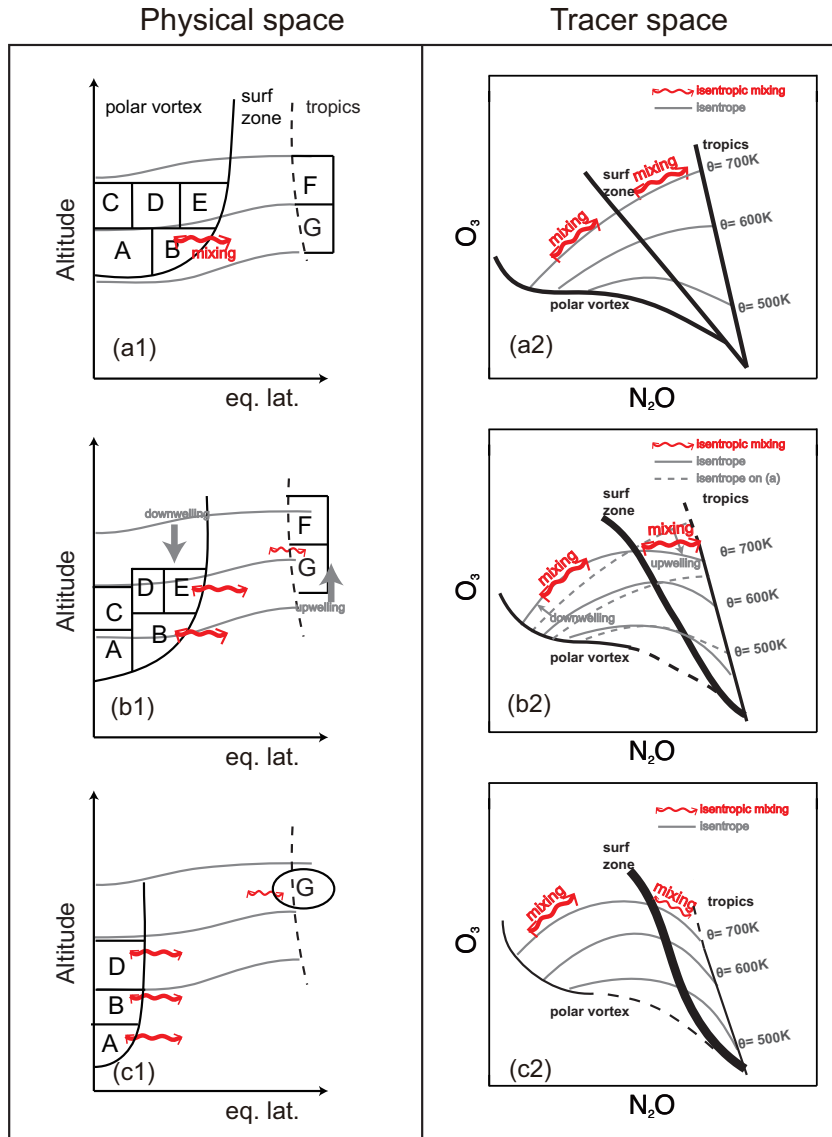


Figure 8. Schematic diagram of transport processes shown in physical space (left column) and tracer space (N_2O - O_3 , right column) before (top), during (middle) and after (bottom) the major SSW. In the physical space (left column), equivalent latitude are used as the horizontal coordinate to illustrate isentropic mixing (curved red arrows) and cross-isentropic transport (gray vertical arrows). The characters denote exemplary the vortex and tropical air masses which interact with the mid-latitude air. Black curves in (a2)-(c2) show respective N_2O - O_3 correlations. Grey lines denote the isentropic levels. In the tracer space, the position of isentropes before (dashed) and after (solid) the major SSW is also marked. The change of the position of a prescribed point in the tracer space along the isentropes quantifies isentropic mixing whereas motion relative to these isentropes describes the effect of an idealized (mixing-free) cross-isentropic motion (up- or downwelling). Changes of the relative thickness of the different correlation branches mean their enhanced or weakened relative contributions to the composition of the considered part of the atmosphere (dashed indicates a possible missing part).

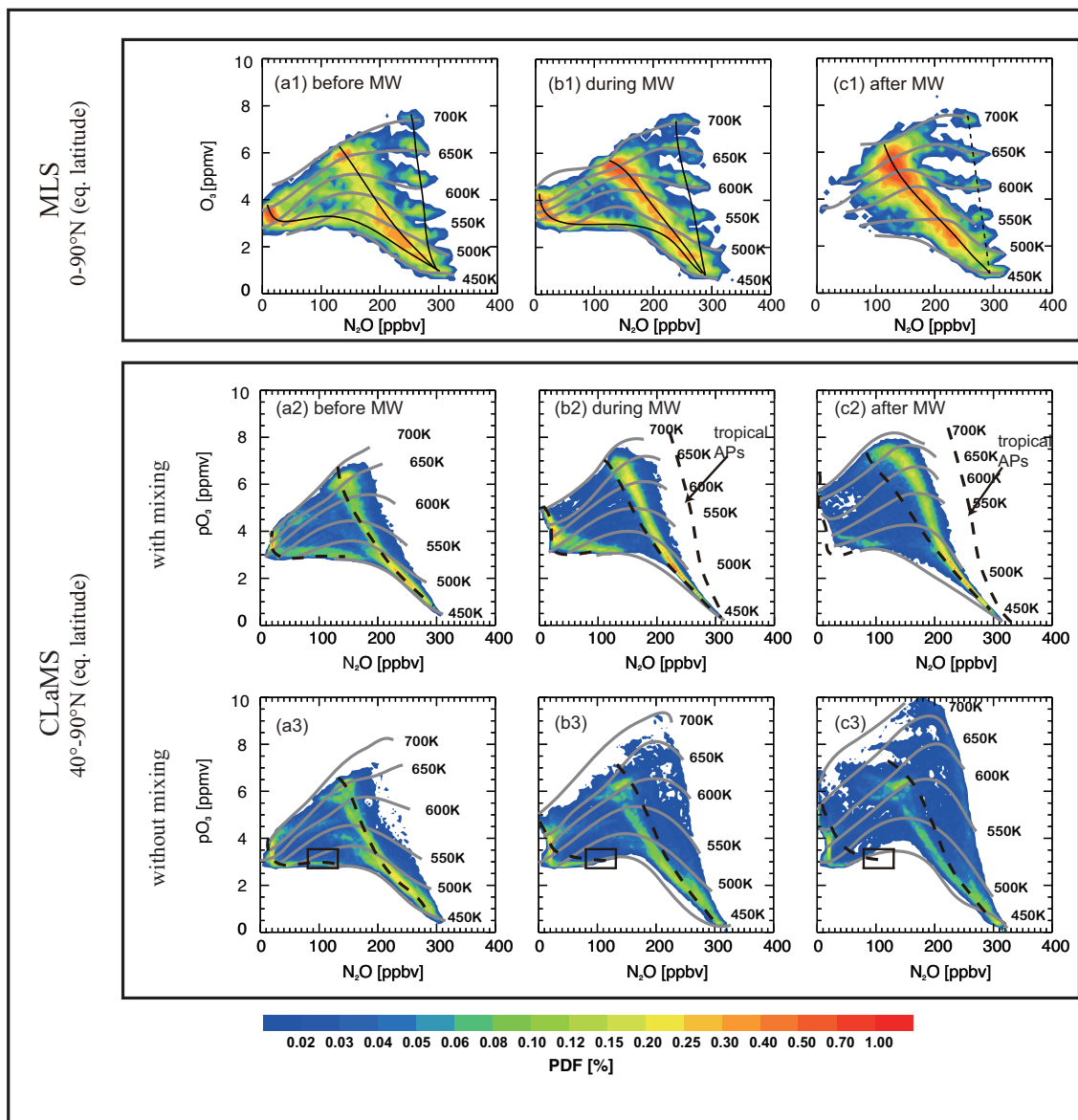


Figure 9. PDFs of N_2O - O_3 correlations (tracer space) shown for 3 periods: (a) December 18-28th, (b) January 18-28th, (c) February 18-28th. Top row (a1-c1) is based on the MLS observations within eq. latitudes 0 - $90^\circ N$ and potential temperature range between 450 and 700 K. The black lines in (a1-c1) represent the respective correlation branches (polar, surf-zone, tropics). Middle and bottom rows show CLaMS simulations without ozone chemistry but with and without mixing, respectively. CLaMS PDFs are calculated from the APs with the same potential temperature range but with eq. latitudes between 40 and $90^\circ N$. The gray lines mark the isentropes (450 , 500 , 550 , 600 , 650 , and 700 K). **For better comparison between CLaMS with and without mixing, the dashed black curves in (a2-c2) show the estimated N_2O - O_3 correlation line from the case without mixing (i.e. from a3-c3). Reversely, dashed lines in (a3-c3) are schematically transferred correlation branches from CLaMS with mixing (i.e. from a2-c2).**

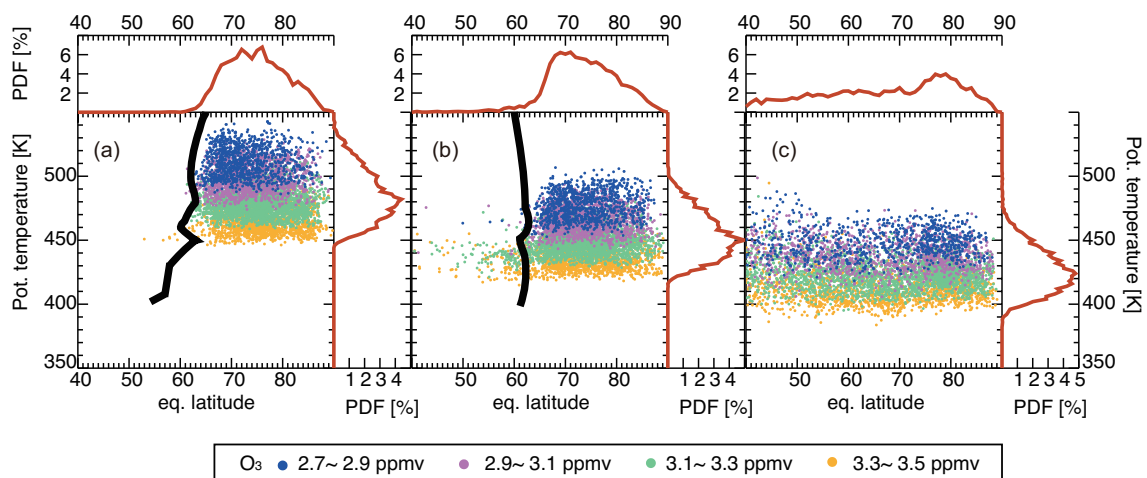


Figure 10. Spatial distribution in the eq. latitude- θ space of the APs defined by the mixing ratios of N_2O and pO_3 inside the square in Fig. 9(a3), i.e. with N_2O and pO_3 values from 80 to 130 ppbv and from 2.7 to 3.5 ppmv, respectively, calculated from CLaMS run without mixing. (a) Dec. 23, 2008; (b) Jan. 23, 2009; (c) Feb. 23, 2009. Colors indicate different ranges of pO_3 values and are defined in the box. The PDFs along the eq. latitude and potential temperature axes are shown as red lines. Thick black lines denote the edge of the polar vortex.

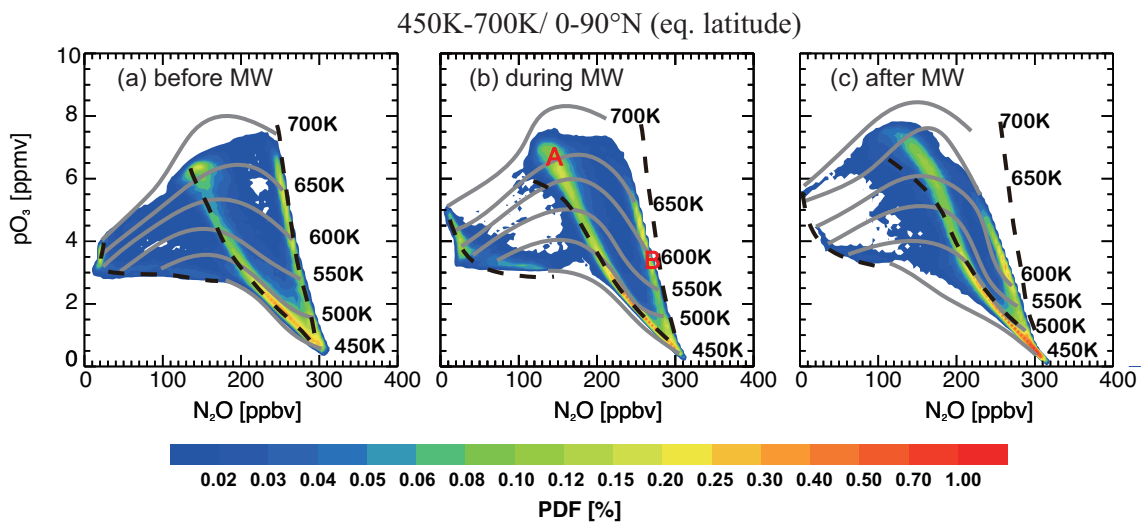


Figure 11. Impact of O_3 -chemistry on the temporal evolution of the N_2O - O_3 correlations. The PDFs are calculated from the N_2O - pO_3 correlations of APs with eq. latitudes 0 - $90^\circ N$ and potential temperatures 450 - 700 K. The considered time periods are the same as in Fig. 9. The dashed black curves fit the maxima of the N_2O - O_3 correlations (PDFs) derived from a CLaMS run with a full stratospheric ozone chemistry. The correlation for passive ozone (pO_3) marked as A (N_2O near 140 ppbv and pO_3 near 7400 ppbv) and the correlation marked as B (N_2O near 140 ppbv and pO_3 near 7400 ppbv) show clear differences from the dashed curves showing simulation with full chemistry. The two groups of APs marked by those correlation features have been investigated in more detail of their ozone chemistry (see text).

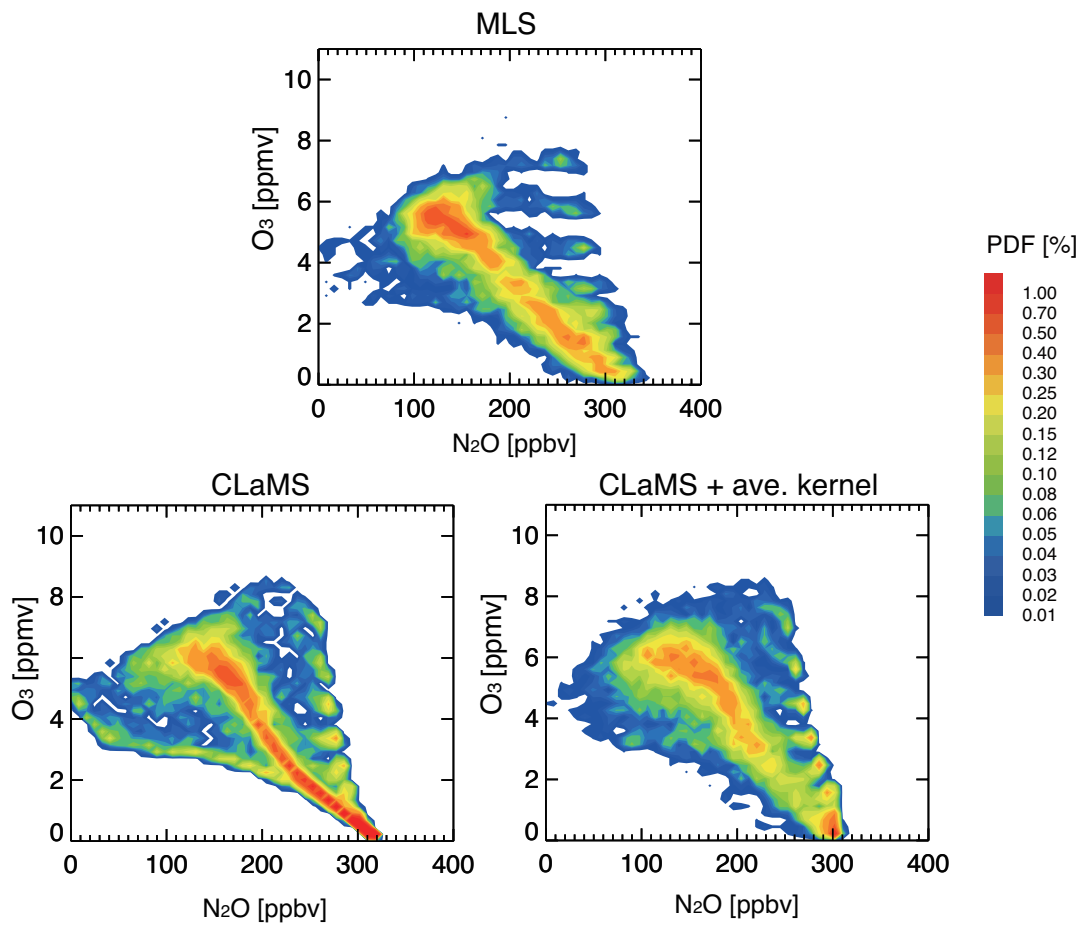


Figure 12. PDFs of N₂O-O₃ correlations on February, 15th, 2009 from MLS observations (top); from the reference CLaMS simulation without applying the averaging kernel (bottom left) and after applying the averaging kernel (bottom right).

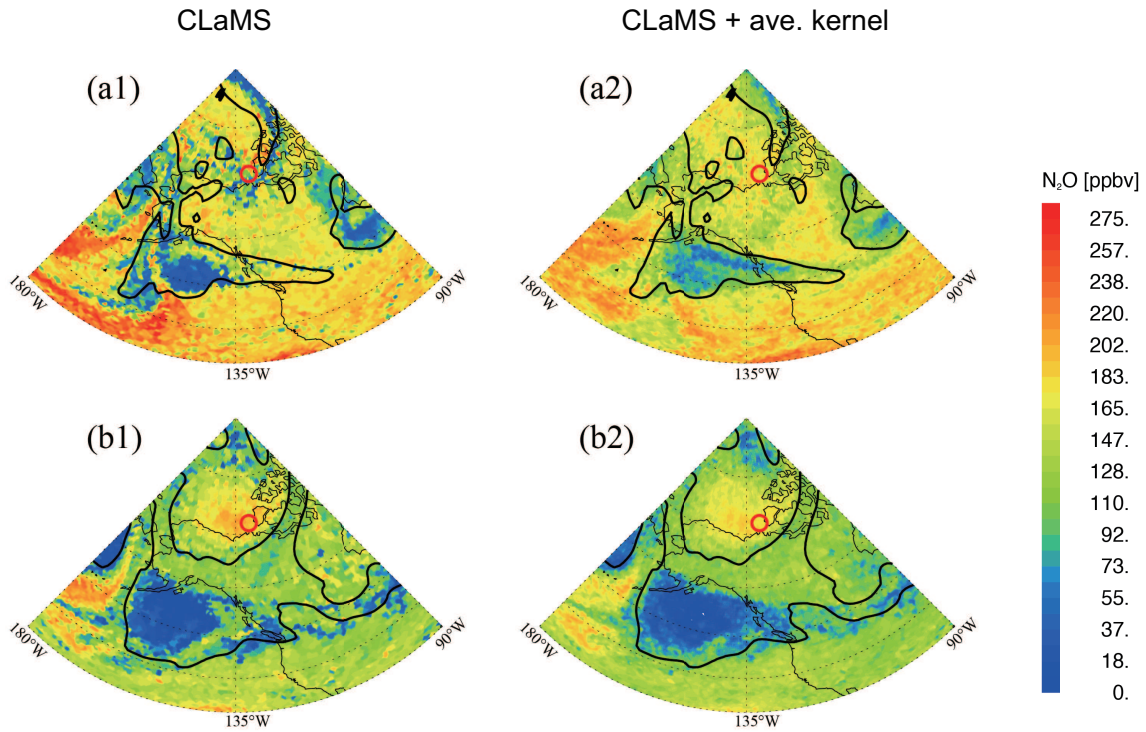


Figure 13. Spatial distribution of N_2O on February, 20th, 2009, i.e., almost 1 month after the major SSW at $\theta = 550$ K (top row) and 650 K (bottom row). Here the results of the reference run without and with the averaging kernel are shown in the left and right column, respectively. Black line is vortex edge, the red circles are the noon-footprints calculated by the observed ACE profile through back and forward trajectory.

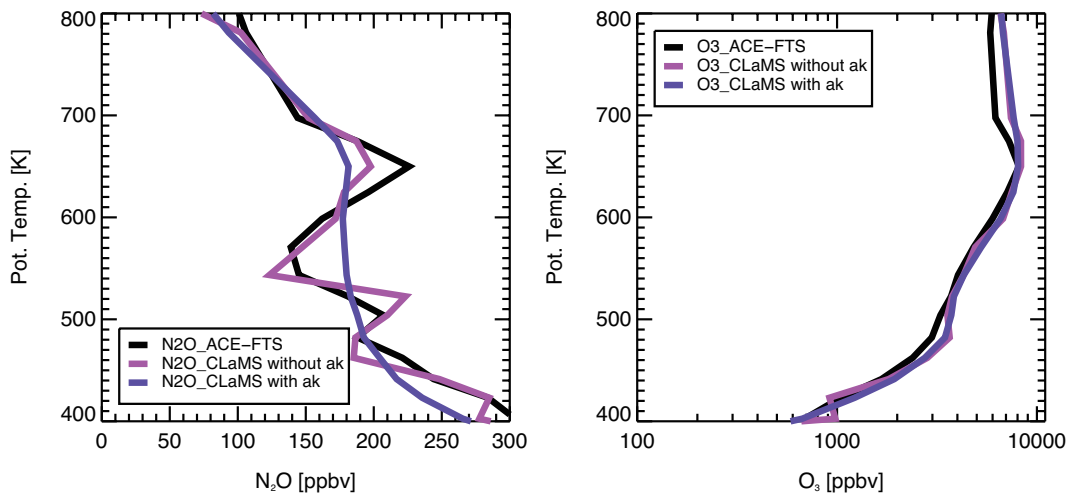


Figure 14. N_2O (top) and O_3 (bottom) profiles of ACE observations (black) on Feb. 20th located at $73.05^\circ N$, $137.11^\circ W$ at 30 km and of corresponding CLaMS simulation before (blue) and after (purple) applying the MLS averaging kernel.